[American Journal of Science, Vol. 311, June, 2011, P. 528–572, DOI 10.2475/06.2011.03]

STRATIGRAPHIC CONTEXT, GEOCHEMICAL, AND ISOTOPIC PROPERTIES OF MAGMATISM IN THE SILURO-DEVONIAN INLIERS OF NORTHERN MAINE: IMPLICATIONS FOR THE ACADIAN OROGENY

ADAM SCHOONMAKER*, WILLIAM S. F. KIDD**, DOUGLAS N. REUSCH***, MICHAEL J. DORAIS§, THOMAS GREGG***, and CHRISTOPHER SPENCER§

ABSTRACT. This paper reports detailed stratigraphic analysis, whole rock geochemistry and Nd isotopic ratios of basalts from the northern Maine inliers. These data place constraints on first-order controversies about the tectonic conditions leading up to and during the early stages of the Acadian Orogeny in northern Maine. Late Silurian and early Devonian stratigraphic sequences indicate a progressive change from shallow water and subaerial exposure (Ripogenus and The Forks formations, East Branch Group) to a rapidly subsiding basin prior to the onset of Acadian deformation. Subsidence was accompanied by mafic to intermediate volcanism of the West Branch, Spider Lake, and Fish Pond volcanics, and that continued with intrusion of the syn-deformational Greenville Plutonic Belt, including the Flagstaff Lake Igneous Complex, whose properties we report in this paper. Trace element geochemistry indicates that magmatism is transdiscriminant, showing aspects of within-plate, volcanic arc, and back-arc affinities and Nd isotopic ratios are moderately positive (+2.3 to +3.8) indicating either an uncontaminated and moderately enriched mantle source, or a depleted mantle source contaminated by continental crust.

Four possible tectonic models of the Acadian Orogeny and the Siluro-Devonian sedimentary-volcanic sequences of northern Maine are evaluated in the context of a subsiding basin associated with this magmatism developed on the amalgamated Laurentian plate. These include 1) slab detachment during southeast-directed subduction of the Laurentian continental margin; 2) "Laramide-style" thrust basins above a shallow, northwest-dipping subduction zone; 3) back-arc extension followed by thin-skinned shortening above a northwest-dipping subduction zone; and 4) "Moluccan-style" dual-dipping subduction zones.

Key words: Acadian orogeny, Piscataquis Volcanic Belt, Piscataquis arc, Acadian magmatism, northern Maine, trace element geochemistry, Nd isotopes, Ripogenus, Acadian subduction polarity, Chesuncook, Munsungun, Lobster Mountain, West Branch

INTRODUCTION

For decades, first order questions regarding the nature of Acadian orogenesis have proved difficult to answer with reasonable certainty. Contrasting ideas regarding the polarity of Acadian subduction and tectonic regime leading up to collision of the Avalon microcontinent with amalgamated Laurentia have been presented in the literature (Bradley, 1983; Robinson, 1993; Bradley, 1993; Keppie and Dostal, 1994; Robinson and others, 1998; van Staal and others, 1998; Murphy and others, 1999; Bradley and others, 2000; Eusden and others, 2000; Tucker and others, 2001; Bradley and Tucker, 2002; Schoonmaker and others, 2005; West and others, 2007; van Staal and others, 2009; Hibbard and others, 2010) without widespread consensus. We present new geochemical and isotopic data, and review existing stratigraphic and geochemical data from the northern Maine region for the period leading up to and

* Department of Geosciences, Utica College, Utica, New York 13502; adschoonmaker@utica.edu
** Department of Atmospheric and Environmental Sciences, University at Albany, Albany, New York 12222
*** Geology Department, University of Maine at Farmington, Farmington, Maine 04938
§ Department of Geological Sciences, Brigham Young University, Provo, Utah 84602

during the Acadian orogeny, and evaluate four tectonic models in the context of these data. We present expanded geochemical (briefly described in Schoonmaker and others, 2005) and new Nd isotopic data of the pre-Acadian, late Silurian to early Devonian mafic volcanic rocks from the Chesuncook Dome, and new geochemical data from the mafic volcanic and intrusive rocks from The Forks and Flagstaff Lake areas of the Lobster Mountain Anticlinorium. The magmatic rocks form part of the Piscataquis magmatic belt, which includes the more temporally restricted Piscataquis Volcanics Belt of Osberg and others (1989), a regionally significant feature more than 1000 kilometers long in the northern Appalachians of Maine and adjacent Canada (fig. 1). These rocks record the changing depositional environments, magmatic events and tectonic conditions during the late Silurian and early Devonian, before and during the early stages of Acadian deformation, which in central northern Maine has been tightly constrained to the Early Emsian stage of the Devonian (408-406 Ma) by Bradley and Tucker (2002).

The nature of the volcanic rocks, both in their geochemical characteristics (especially whether or not they have an arc affinity), and their tectonic setting as recorded by the enveloping stratigraphic associations, is significant not only for the tectonics during the Acadian orogenic event, but more generally, to the context of mafic magmatism in the area near a migrating convergent thrust deformation front.

GEOLOGY OF THE NORTHERN MAINE INLIERS (PRE-SEBOOMOOK FORMATION)

Deposition of the Seboomook Formation marks the onset of the Acadian orogeny in the northern Maine inliers (Bradley and others, 2000). The relationships between the sedimentary and volcanic rocks of the underlying pre-Seboomook sequence of northern Maine are discussed below to demonstrate that they were in geographic proximity during the Acadian Orogeny. Inliers examined here include the Lobster Mountain, Weeksboro-Lunksoos, and Munsungun anticlinoria (fig. 1) and their stratigraphic relationships are summarized in figure 2. All occur southeast of the Red Indian Line (Hibbard and others, 2006), have a peri-Gondwanan connection based on Celtic fossil assemblages in the Weeksboro-Lunksoos Anticlinorium (Neuman, 1984), and along-strike Acadian plutons have Gondwanan isotopic signatures (Dorais and Paige, 2000). They are composed of deformed late Precambrian or early Cambrian through Ordovician low-grade metasedimentary rocks, mafic meta-volcanic rocks, and meta-gabbro, which are unconformably overlain by less deformed late Silurian–early Devonian shallow to deep marine sedimentary rocks and volcanics of the Piscataquis Volcanic Belt (as defined by Osberg and others, 1989); all are onlapped by Devonian Seboomook Flysch and intruded by Acadian granitic and mafic plutons of the Greenville Plutonic Belt (Osberg and others, 1985).

Pre-Silurian Rocks and Middle Ordovician/Silurian(?) Angular Unconformity

In all of the northern Maine inliers, middle to late Ordovician rocks are truncated by an erosional unconformity that has been inferred to be Taconic in origin (Griscom, ms, 1976; Hanson and Bradley, 1989; Kusky and others, 1994; Schoonmaker and Kidd, 2006), although direct, and closely time-constraining evidence for this is lacking. It is possible that this unconformity is in part or wholly a product of the Silurian Salinic orogeny (for example, van Staal and de Roo, 1995), although its age predates the original Salinic "disturbance" originally defined by Boucot (1962).

In the Chesuncook Dome The Dry Way Volcanics are unconformably overlain by the Ripogenus Formation. The Bean Brook Gabbro, with a K/Ar age of 473 Ma (recalculated from Faul and others, 1963), is considered to be the intrusive equivalent to the Dry Way Volcanics. Ludlovian to lowermost Lockhovian conodonts occur in the Ripogenus Formation above the unconformity in the Ripogenus Gorge (Bradley and others, 2000).

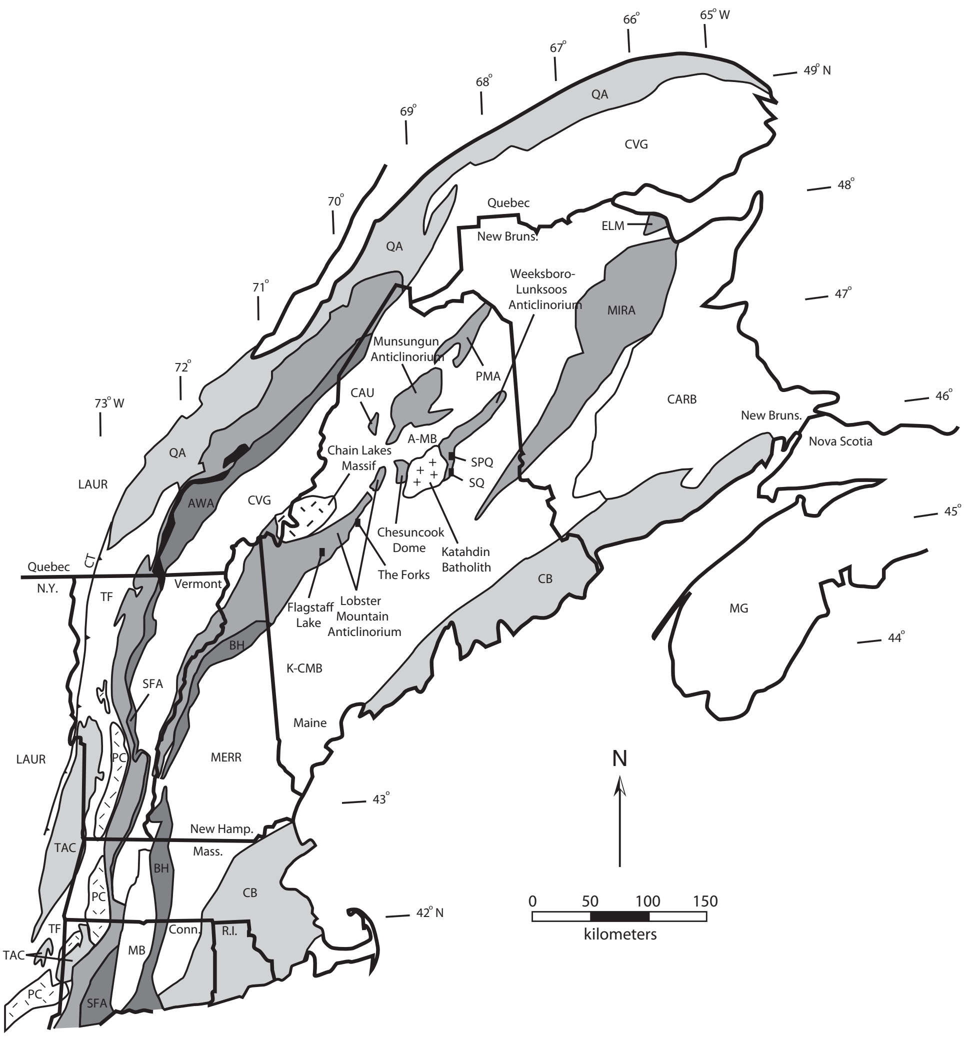

Fig. 1. Generalized geology of the northern Appalachians. Pre-Devonian units are shaded. LAUR = autochthonous Laurentian margin, QA = Quebec Allochthons, TAC = Taconic Allochthons, TF = transported Laurentian margin and basin deposits, PC = Precambrian massifs, SFA-AWA = Shelburne Falls arc, Ascot-Weedon arc, and related oceanic rocks, including ophiolitic fragments (black), MB = Mesozoic basin, CVG = Connecticut Valley Gaspe Synclinorium, BH = Bronson Hill Arc, MERR = Merrimack Synclinorium, CAU = Caucomgomoc inlier, A-MB = Aroostook-Matapedia belt, SPQ = Shin Pond quadrangle, SQ = Stacyville quadrangle, PMA = Pennington Mtn. Anticlinorium, MIRA = Miramichi Highlands, K-CMB = Kearsarge–Central Maine belt, ELM = Elmtree-Belledune inlier, CARB = Carboniferous cover rocks, CB = Coastal belt, MEG = Meguma terrane. Adapted from Williams (1978), Osberg and others (1985), and Robinson and others (1998).

In the Lobster Mountain Anticlinorium, Boucot (1969) and Simmons (1987) reported slate, phyllite and graywacke and volcanic rocks of Cambrian or Ordovician age that are nearly vertical in attitude. Although the contact is not observed, the overlying Lobster Lake Formation is less deformed and contains pebbles of volcanics from the underlying units. Based on this relationship, Boucot (1962, 1969) inferred the presence of an unconformity and suggested that it correlates with the angular unconformity seen in the Ripogenus Gorge. Nearby, Marvinney (1984) introduced the

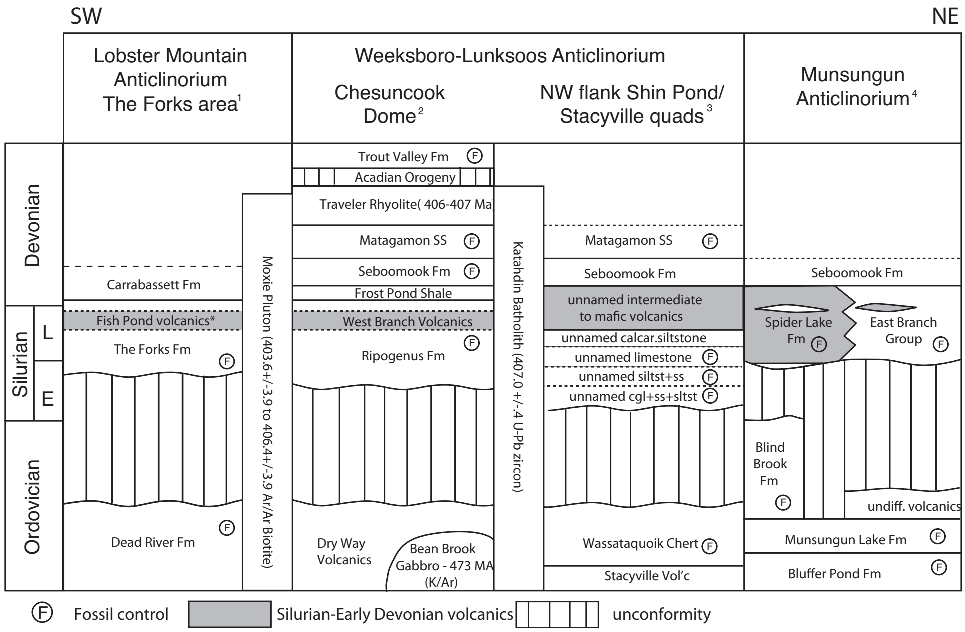

Fig. 2. Correlation chart of Ordovician through Devonian rocks of north-central Maine. Igneous ages from Faul and others, 1963; Rankin and Tucker, 1995; and Bradley and others, 2000. Compiled from: [1]Marvinney, 1982, 1984; Burroughs and Marvinney, 1981; [2]This study, Griscom (ms, 1976), Jarhling (1981, cited in Boone and Boudette, 1989), Osberg and others (1985), and Rankin and Hon (1987); [3]Neuman (1967); [4]Hall (1970).

name "The Forks Formation" for a transgressive sequence of lower carbonate-rich rocks and upper siliciclastic beds that had been previously assigned to the Ripogenus Formation by Griscom (ms, 1976). These unconformably overlie more deformed Cambro-Ordovician rocks and Marvinney suggested a correlation of this unconformity with the Taconian or Penobscottian unconformities, but this also may alternatively be Salinic.

In the Munsungun Anticlinorium, pillowed mafic greenstones of the Bluffer Pond and Munsungun Lake formations (Ashgill graptolites) are correlated with the Cambrian to Ordovician metasedimentary rocks in the Chesuncook Dome (Hall, 1970; Griscom, ms, 1976; Schoonmaker and Kidd, 2006). These are separated from overlying Siluro-Devonian rocks by an angular unconformity that Hall (1970) attributed to the Taconic Orogeny and is likely equivalent to the unconformity seen in the Ripogenus Gorge.

In the Shin Pond–Stacyville area of the Anticlinorium, the Ordovician Stacyville Volcanics and Wassataquoik Chert (conodonts and graptolites reported as Normanskill age) are truncated by an erosional unconformity (Neuman, 1967). Neuman (1967), Hall (1970), and Griscom (ms, 1976) all considered the Stacyville, Bluffer Pond, and Dry Way Volcanics equivalent and this correlation is supported by their similar geochemistries (Winchester and van Staal, 1994; Schoonmaker and Kidd, 2006). The unconformity above the Stacyville Volcanics is therefore likely equivalent to the Ripogenus Gorge unconformity. There is, additionally, a structural contrast between the highly deformed, late Precambrian to early Cambrian Grand Pitch Formation and overlying, less-deformed, latest Early Ordovician or earliest Middle Ordovician Shin Brook Formation in the Weeksboro-Lunksoos Anticlinorium, from the Penobscottian event (Neuman, 1967).

These age constraints suggest that the pre-Silurian rocks of the northern Maine inliers and the Chain Lakes Massif were amalgamated into the Laurentian margin and uplifted to erosion in latest Ordovician or early Silurian time. A late Ordovician interpretation would place this at about the time of Bronson Hill magmatism. An early Silurian interpretation places it near the time of Salinic orogenesis (for example, van Staal and others, 2009).

Latest Silurian to Earliest Devonian Shallow Marine Deposition

In the Ripogenus Gorge section of the Chesuncook Dome, the Ripogenus Formation is nearly continuously exposed and overlies the Taconic/Salinic unconformity in the Chesuncook Dome. It is a heterogeneous unit that includes conglomeratic arenite at its base progressively overlain by nodular calcareous arenites, discontinuous orthoquartzite, fossiliferous limestone, and limestone breccia (fig. 3). The formation is Late Silurian to earliest Devonian in age, based on Wenlock- to Ludlow-aged brachiopods (Griscom, ms, 1976) in the nodular calcareous sandstone, and a late Ludlow to early Lockhovian suite of conodonts reported by Bradley and others (2000) from bedded limestones directly above the discontinuous orthoquartzite in the section.

In the Lobster Mountain Anticlinorium, The Forks Formation (Marvinney, 1984) includes a carbonate-rich lower sequence of shallow marine rocks with a basal conglomerate conformably overlain by an upper siliciclastic sequence (fig. 4). This unit had been previously correlated with the Ripogenus Formation and most likely represents the lower (sub-orthoquartzite) section although age confirmation is lacking.

Above the Taconic/Salinic unconformity in the Munsungun Anticlinorium, Siluro-Devonian rocks of the East Branch Group (Carpenter Pond, Chandler Pond, and Third Lake formations) and the Spider Lake Formation (Hall, 1970) occur. Fossil assemblages reported as Pridoli (possibly Ludlow) to Helderberg age occur mainly in the Third Lake and Spider Lake formations (Hall, 1970). The units of the East Branch Group have a complex stratigraphic and geographic relationship (fig. 5) with lenses of Chandler Pond occurring both above and below the other two units. Hall (1970) interpreted the lower part (lower Chandler Pond Formation to Third Lake Formation) to be a transgressive sequence. The Chandler Pond Formation is a conglomerate and contains fragments of the underlying Ordovician rocks, while the Third Lake Formation contains reefal limestones, siltstones, and limestone breccias. The Spider Lake Formation is dominated by andesitic flows interstratified with sediments similar to those of the Third Lake Formation, but has a basal conglomerate that may be correlative with the lower Chandler Pond Formation. The Chandler Pond Formation and basal conglomerate of the Spider Lake Formation are of the same approximate age (Hall, 1970) and occur in the same stratigraphic position as the lower Ripogenus Formation.

In the Shin Pond–Stacyville area, unnamed Silurian (late Llandovery) conglomerates, sandstones, siltstones, and reefal limestones unconformably overlie the Ordovician rocks. The basal conglomerates are considered by Griscom (ms, 1976) to be equivalent to the basal Ripogenus Formation and he also reports the reefal limestones in the Shin Pond–Stacyville area to be nearly identical to the limestone section of the Ripogenus Formation.

Disconformity Within the Shallow Marine Section

Begeal and others (2004) identified the base of the orthoquartzite in the Ripogenus gorge (fig. 3) as an erosional surface and sequence boundary, representing a period of emergence. The white orthoquartzite is composed almost entirely of well-cemented, sub-angular to well-rounded, fine- to medium-grained quartz sand. In the Ripogenus Gorge and vicinity, the unit has highly variable thickness over short

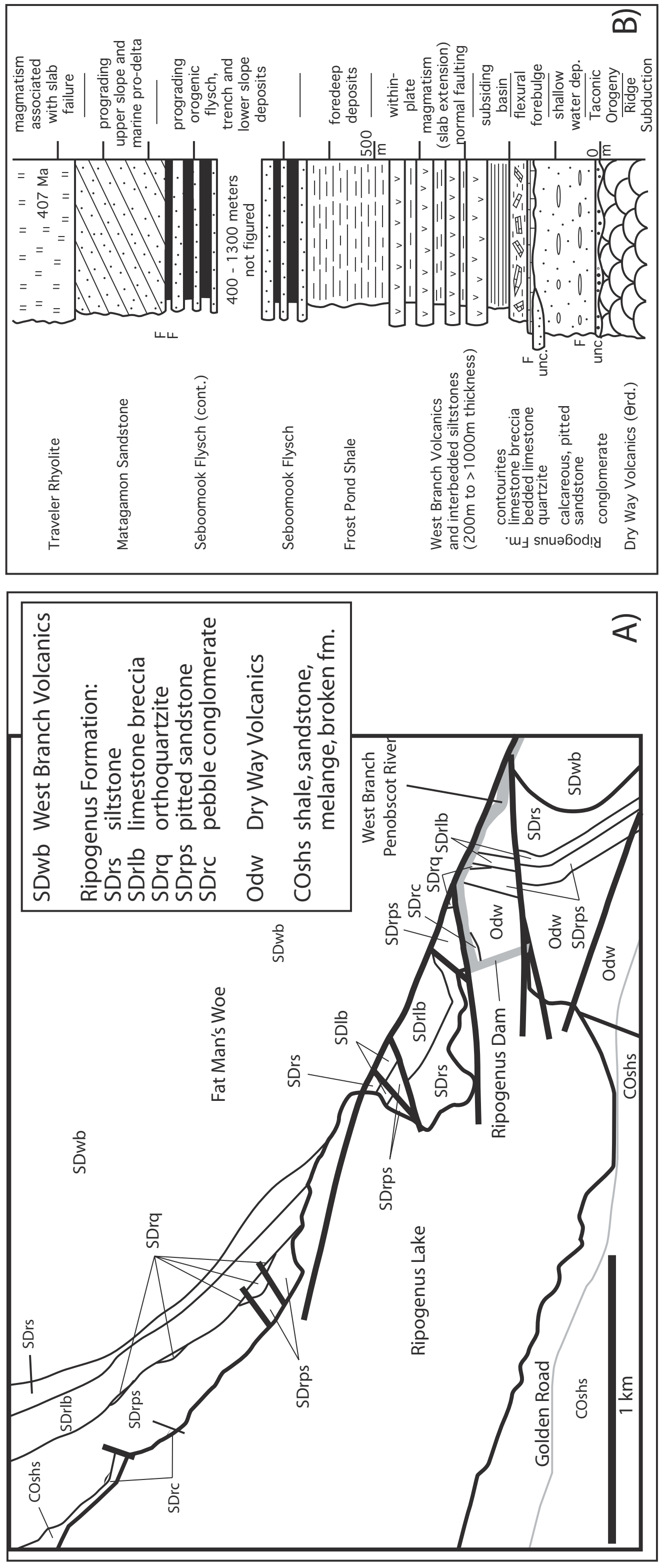

Fig. 3. Geology of the Ripogenus Gorge area, Chesuncook Dome. (A) Geologic map of area surrounding the gorge. Heavy lines indicate faults. Adapted from Begeal and others (2004). (B) Stratigraphic column of the exposed section in the Ripogenus Gorge (from Schoonmaker and others, 2005).

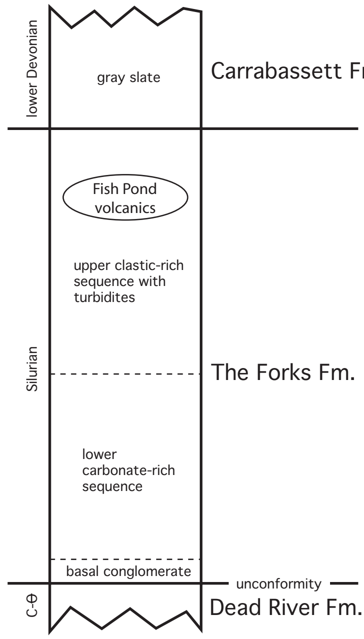

Fig. 4. Stratigraphic column of The Forks Formation (based on Marvinney, 1984, and Burroughs and Marvinney, 1981).

distances, from locally absent up to a maximum thickness of about 18 meters, and is interpreted to be filling paleotopography eroded into the underlying calcareous arenites. Overlying the orthoquartzite in the Ripogenus Gorge is a thin (1-2 meters) bedded, conodont-bearing (late Ludlow to early Lockhovian) limestone overlain by a thicker (up to 50 meters) limestone breccia. Some exposures show the underlying

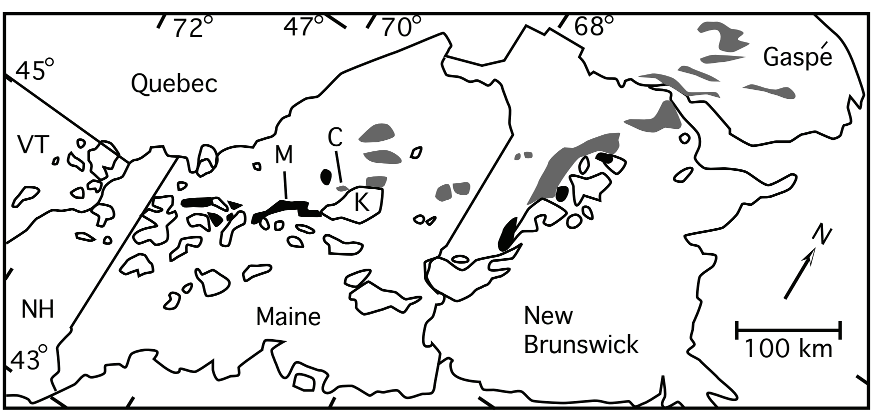

Fig. 5. Regional map showing distribution of Silurian-Devonian magmatism. Open fields = granitoid plutons; black = mafic plutons; gray = volcanics, mainly basaltic and andesitic; K = Katahdin batholith; M = Moxie pluton; C = Chesuncook Dome. Dashed line is general trace of magmatic belt. Adapted from Williams (1978); Dostal and others (1979), and Bradley and others (2000).

bedded limestone grading upward into breccia, with some clasts in excess of two meters across (Begeal and others, 2004).

Evidence for this erosion surface has also been reported in the Munsungun Anticlinorium where Hall (1970) reported a horizon of conglomerate in the Chandler Pond Formation of the East Branch Group containing variable clasts of coeval and older lithologies, including volcanic clasts interpreted to represent a short period of sub-aerial exposure of post-Pridolian age.

A similar event may also be recorded in the northwestern sequence of the Weeksboro-Lunksoos Anticlinorium, where Neuman (1967) described a polymict conglomerate occurring within calcareous siltstone of Late Silurian age, near White Horse Lake. He inferred a localized, relatively short infusion of terrigenous material during a period of transgression.

Boucot (1962, 1969) inferred an erosional event between Silurian and Devonian rocks in the Lobster Mountain Anticlinorium, which he termed the "Salinic Disturbance," based on the discontinuous nature of Silurian units beneath the Devonian stratigraphy. It is possible that some or all of this discontinuity is an equivalent feature to the disconformity in the Ripogenus section of the Chesuncook Dome, but is not time equivalent with the angular unconformity at the base of the Ripogenus Formation.

Pre-Seboomook Sedimentary Rocks and Mafic to Intermediate Volcanic Rocks

The limestone breccia in the Ripogenus Gorge conformably underlies purple siltstone (a green hornfels in the vicinity of the Katahdin Granite in the Ripogenus Gorge) interstratified with thin, laterally persistent, fine-grained, laminated white quartz arenites and silts that are interpreted to be contourites (Begeal and others, 2004). The thin beds, a few millimeters to a centimeter thick, and their sharp contacts with enclosing siltstones, are persistent across the outcrop for distances of tens of meters. The siltstone is inferred to grade upward into the Frost Pond Shale, a geographically widespread, fine-grained, red argillite that varies in thickness from about 30 to 200 meters and is largely featureless (Griscom, ms, 1976), and which is in turn overlain by the Seboomook Formation. The West Branch Volcanics are interstratified with siltstones identical to those of the upper Ripogenus Formation; Griscom (ms, 1976) identified the base of the lowest volcanic unit as the top of the Ripogenus Formation (fig. 3). The volcanics are basalt, basalt-andesite, and andesite; the latter locally contain silicic inclusions (Griscom, ms, 1976; Fitzgerald, ms, 1991; Schoonmaker and others, 2005). They have been interpreted to be flows, although some horizons may be sills. Most flows are massive, some are crudely columnar-jointed and a few are clearly pillowed. The volcanics occur above the conodont-bearing horizons identified by Bradley and others (2000), which have a Late Ludlow to early Lockhovian age. The whole rock geochemistry and Nd isotopic ratios of the West Branch Volcanics and their correlatives are discussed below.

The upper part of The Forks Formation in the Lobster Mountain Anticlinorium is composed of an arenite-dominated sequence of turbidites (Marvinney, 1984). Within this sequence are lenticular bodies of vesicular and pillowed mafic volcanics (Fish Pond volcanics) in a similar stratigraphic position as the West Branch Volcanics (fig. 4). Overlying The Forks Formation is the Carrabassett Formation, a dark gray slate with thin beds of graywacke (Burroughs and Marvinney, 1981) and probably correlative with the basal unit of the Seboomook Formation (for example, Moench, 2006). Near Moosehead Lake, the Capens Formation and Whiskey Quartzite, which Marvinney (1984) correlated with The Forks Formation, occur between unnamed Silurian strata of Boucot (1969), and beneath the Seboomook Formation. Boucot (1969) tentatively correlated the red slate of the Capens Formation with the Frost Pond Shale and interpreted the limited exposure of the overlying quartzite to a local topographic high.

Given that similar lithologies do not occur at this stratigraphic position in the other inliers, this is a reasonable inference.

In the Munsungun Anticlinorium, the upper part of the East Branch Group is composed of calcareous siltstones, limestones, and limestone breccias of the Third Lake Formation (Hall, 1970). He reported fossil debris horizons and discontinuous allochthonous (sedimentary) beds. The age of these rocks is lower Devonian (Helderberg) based on fossil assemblages collected by Hall (1970). Similar horizons are found interstratified with the volcanics of the Spider Lake Formation and this shows that extrusion of Carpenter Pond and Spider Lake volcanics is at least in part synchronous with Third Lake Formation deposition. These units occur in a stratigraphic position similar to the West Branch Volcanics. Fitzgerald (ms, 1991) determined the geochemistry of the volcanic rocks of the Spider Lake Formation and the results are reviewed in detail below.

In the Shin Pond–Stacyville area, Neuman (1967) mapped a thick (>150 m) late Silurian (early Ludlow) calcareous siltstone between underlying reefal limestones and overlying intermediate to mafic volcanic flows of late Silurian or Early Devonian age. Griscom (ms, 1976) considered these units to be equivalent to the Ripogenus siltstones and West Branch Volcanics. However, no geochemical analyses have been reported for these volcanics.

Discussion of Siluro-Devonian Stratigraphy

Collectively, these basal Silurian coarse-clastic and reefal limestones above the late Ordovician–early Silurian (Taconic/Salinic?) angular unconformity indicate shallow water deposition in an initially near shore, overall shallow marine environment during late Silurian to early Devonian time. This likely occurred on the Ganderian crust, accreted to Laurentia (van Staal and others, 2009). Isotopic evidence from Devonian plutons from other parts of Maine, both along-strike and to the southeast shows Gondwanan affinities indicating Ganderian crust underlies this part of the orogen (for example, Pressley and Brown, 1999; Dorais and Paige, 2000). Deposition was at least locally interrupted by a period of sub-aerial exposure marked by the white orthoquartzite in the Ripogenus Gorge and conglomerates in the other inliers. The Ripogenus Gorge provides unusually good outcrop including a nearly continuous section, and the local area has been mapped in full outcrop detail (Begeal and others, 2004), so the stratigraphy is confidently established. However, the stratigraphic relationships in the Munsungun Anticlinorium are less clear due to poor exposure. Faulting or other unidentified structures may complicate or invalidate our current understanding of the Munsungun East Branch Group stratigraphic relationships.

The limestone breccias near the top of the Ripogenus Formation indicate a disturbance, possibly the initiation of significant tectonic activity in the area, and it immediately precedes a rapid change in the pattern of sedimentation from shallow marine coarse-clastic and carbonate to fine-grained clastic rocks of the Ripogenus siltstones, turbidites of The Forks Formation, and Frost Pond Shale. Minor normal faults have been observed cutting the Ripogenus Formation, which may be related to this activity. This is also accompanied by volcanism of the West Branch Volcanics and correlatives. Griscom (ms, 1976) inferred an estuarine environment for the Frost Pond Shale, taking its red (oxidized) color as indicating a shallow water origin with episodic sub-aerial exposure. However, the shale is monotonously featureless and lacks many of the primary structures that might be expected in such an environment, including bioturbation, channels, crossbeds, shallow marine fossils, evidence for episodic regressions and periods of emergence, or other shallow water features. Further, the lack of disruption of thin contourites in the underlying upper Ripogenus Formation argues for a more distal, deeper water depositional environment, as does the conformable passage from the Frost Pond Formation up into the basal turbidites of the Seboomook

Formation. The lower sand-dominated Ripogenus Formation represents shallow water deposition; we argue that following deposition of the orthoquartzite water depth increased rapidly, resulting in the deposition of silty contourites of the Ripogenus Formation, turbidites of the upper part of The Forks Formation, and Frost Pond Shale in a deep water, sub-wave base environment. We also think that the limestone breccia present directly beneath the silty contourites of the upper Ripogenus Formation may be related to the development of normal fault scarps accompanying the subsidence rate increase evidenced by the major change in facies of these overlying clastic sediments. That mafic volcanism accompanied the initiation of more rapid subsidence is unlikely to be coincidental.

ROCKS OF THE ACADIAN OROGENY

Seboomook Group

Easterly-derived flysch of the Seboomook Group and overlying shallower marine "delta" deposits of the Matagamon Sandstone cover the northern Maine inliers; the former is the first evidence of the Acadian orogenic wedge approaching from the east (Hall and others, 1976; Pollock, 1987; Pollock and others, 1988; Bradley and others, 2000). Both of these units near the Chesuncook Dome contain Pragian brachiopod suites (Griscom, ms, 1976). Similarly, the Seboomook Group near the Munsungun Anticlinorium and Moose River Synclinorium (including the Tarratine Formation) is also of Pragian age (Hall, 1970; Bradley and others, 2000). On the northwest flank of the Weeksboro-Lunksoos Anticlinorium, Neuman (1967) assigned a lower Devonian age to the Seboomook and a Pragian age to the Matagamon Sandstone.

Acadian Magmatic Rocks

The Greenville Plutonic Belt and associated volcanic rocks of the Piscataquis and the Tobique Volcanic belts extend for several hundred kilometers from Massachusetts to New Brunswick (fig. 5) and are generally interpreted to be the result of the Acadian Orogeny (Fyffe and others, 1981; Bradley, 1983).

The Traveler Rhyolite (Rankin, 1968), with 406 and 407 Ma zircon U/Pb ages (Rankin and Tucker, 1995), conformably overlies the Matagamon Sandstone near the Chesuncook Dome. The intrusive equivalent, the Katahdin Batholith (zircon U/Pb age of 406.9 +/− .4 Ma; Rankin and Tucker, 1995) intrudes rocks of the Chesuncook Dome and Weeksboro-Lunksoos Anticlinorium, locally including the Traveler Rhyolite (Neuman, 1967; Griscom, ms, 1976). The mafic Moxie Pluton (404.3 +/− 3.4 [zircon U/Pb] and 406.3 +/− 3.8 Ma [$^{40}Ar/^{39}Ar$]; Bradley and others, 2000) is approximately coeval with Katahdin/Traveler magmatism. Other plutons in the region show similar ages, in a narrow range between 408 to 404 Ma (Hubacher and Lux, 1987; Bradley and others, 2000; see also fig. 3 of Bradley and Tucker, 2002). Some plutons truncate Acadian folds, while syn-tectonic relationships are observed in others (Bradley and Tucker, 2002).

To the southwest, Nielsen and others (1989) describe the ~400 Ma Flagstaff Lake Igneous Complex as consisting of three main rock types: gabbro, granite, and garnet tonalite, with minor trondhjemite. Over 60 percent of the complex was mapped as gabbro that forms two separate bodies along the northeastern and southwestern portions of the complex (see fig. 1 of Nielsen and others, 1989). Approximately 1/3 of the complex consists of a two-mica granite that lies between the two gabbroic bodies. Small bands of garnet tonalite lie within the southwestern portions of the gabbro. Nielsen and others (1989) interpreted this heterogeneity to be the result of magma mixing of a mantle-derived gabbroic body with granitic melts from the country rock. Garnet tonalite and trondhjemite are associated with magma/wall rock interfaces and may represent interaction between crystallizing magmas and wall rocks.

The abundant magmatism in northern Maine during this interval is bimodal. Several authors (Hon, 1980; Rankin and Hon, 1987; Bradley and Tucker, 2002; Schoonmaker and others, 2005) have interpreted the mafic plutons (for example, Moxie) to be the result of partial melting of sub-lithospheric mantle and that heat from these plutons caused partial melting of continental crust to form the granitic melts (for example, Katahdin pluton). This conclusion is supported by intermediate $^{207}Pb/^{204}Pb$, $^{206}Pb/^{204}Pb$ and Sr isotope values in granitic rocks that indicate a mixing of a mafic component into the felsic melts (Ayuso, 1986).

Based on these plutonic ages and observed structural relationships between the intrusive and country rocks, Bradley and others (2000) and Bradley and Tucker (2002) were able tightly to constrain the age of Acadian deformation in this area to the Early Emsian, and in the larger context of a northwesterly migrating deformation front is consistent with the conclusion that the Acadian was locally a short lived event as proposed by Rankin (1994) and Hubacher and Lux (1987).

PETROGRAPHY

The detailed geochemistry described in the next section includes new data as well as previously reported analyses from Fitzgerald (ms, 1991). A summary of the petrography of Fitzgerald's samples is given below, but the reader is referred to that report for detailed descriptions. The petrographic descriptions of new samples are of the West Branch Volcanics from the Ripogenus Gorge and surrounding area, the Fish Pond volcanics in The Forks area, and the gabbroic section of the Flagstaff Lake Igneous Complex.

The West Branch Volcanics are medium-grained tholeiitic basalts and basalt-andesites with a holocrystalline sub-ophitic to ophitic texture. Primary minerals dominate and include subhedral to euhedral, variably saussuritized, Carlsbad twinned plagioclase (An_{30-37}), subhedral to anhedral calcic clinopyroxene, opaques (some skeletal), and rare quartz that may be secondary. No orthopyroxene was observed and any original olivine likely has been altered to chlorite. All samples exhibit greenschist grade metamorphism that includes chlorite, epidote, and calcic amphiboles (actinolite?) and there is some zeolite mineralization in rare veins, including identified natrolite and celadonite. Calcite is occasionally present in small amygdales.

Fitzgerald's (ms, 1991) description of the West Branch Volcanics is similar to that given above, but he reports slightly higher anorthite contents in plagioclase (An_{42-64}). The Spider Lake basalts are finer-grained (although large plagioclase crystals, up to 1 cm may occur locally) relatively homogenous, with primary and alteration mineralogies similar to the West Branch Volcanics, but display intersertal textures, in addition to ophitic and sub-ophitic textures.

The Forks Formation contains dark-green basalt flows that are plagioclase-phyric with an aphanitic groundmass. In several locations, the flows have a vesicular (amygdaloidal) texture. Felsic rocks from dikes contain euhedral grains of quartz and plagioclase feldspar within a felsitic matrix. Both the basalt flows and felsic dikes display secondary chlorite alteration.

A subordinate amount of gabbro is present in the Flagstaff Lake complex. Nielsen and others (1989) report a sample containing ~30 modal percent olivine, whereas most gabbros contain equal proportions of pyroxene and plagioclase with minor amphibole. The mapped southwestern gabbroic unit is dominated by quartz diorites and tonalites. These rocks consist of amphibole, biotite, plagioclase (An_{25-40}), variable amounts of quartz (10-25%) with magnetite, titanite, and apatite as the main accessory phases. Minor chloritization of biotite is present in some samples as is minor saussuritization of the more calcic plagioclase. Most samples are fresh with hypidiomorphic-granular textures. Also present in the gabbro are small intrusions of granite. These are coarser-grained than the quartz diorites and tonalites, containing perthites up to 2 cm long. Unlike the main two-mica granite, no primary muscovite was observed in them.

GEOCHEMISTRY

Whole rock samples of volcanic rocks of the pre-Acadian West Branch, Fish Pond, and Spider Lake formations and plutonic rocks of the syn-Acadian Flagstaff Lake igneous complex were analyzed for major, trace, and rare earth elements. Nd isotopic ratios were determined for five of the West Branch samples.

Previous Work

Fitzgerald (ms, 1991) and Fitzgerald and Hon (1994) analyzed the chemistry of West Branch Volcanics from the Chesuncook Dome and the Spider Lake Volcanics from the Munsungun Anticlinorium, identifying them as "transdiscriminant suites," hypothesizing that they erupted during a transition period between pre-orogenic extension of the Laurentian margin and subsequent compression resulting from collision with the Avalon terrane. Schoonmaker and others (2005) interpreted the geochemistry of the West Branch Volcanics and related Moxie Pluton in the context of correlative Siluro-Devonian stratigraphy that resulted from detachment of the lower plate (east-directed subduction) during the early Acadian Orogeny, building on the ideas proposed by Robinson (1993), Robinson and others (1998), Bradley and others (2000), Tucker and others (2001), and Bradley and Tucker (2002). Gregg and Reusch (2007) reported similar geochemistries from the Siluro-Devonian volcanics in The Forks area. Dostal and others (1989), and Keppie and Dostal (1994) have also proposed related models of magmatism in Maine and New Brunswick involving mantle delamination and transpression, respectively. Nielsen and others (1989) examined the magmatic origin of the ~400 Ma Flagstaff Lake Igneous Complex on the basis of field relations, and petrologic and geochemical data. They concluded that the granite-gabbro complex was emplaced as a result of magma mixing between mantle-derived gabbro and granites formed from the anatexis of country rock, similar to conclusions reached for other coeval bimodal suites (Greenville Plutonic belt) in the region (for example, Hon, 1980; Thompson, 1984; Ayuso, 1986).

The West Branch, Spider Lake, and The Forks suites all represent pre-Acadian magmatism (pre-Emsian), while the Flagstaff Lake intrusive complex was emplaced during Acadian orogenesis in this area.

Trace Element Data Used in This Study

We have compiled 62 whole rock geochemical analyses (table 1) from the late Silurian and early Devonian magmatic belts of northern Maine. Seven analyses referred to, but not described in Schoonmaker and others (2005; laboratory procedures used to complete these analyses, not previously published, are included in Appendix 1) are from the West Branch Volcanics in and near the Ripogenus Gorge (including the cliffs of Fat Man's Woe). Analyses made by Fitzgerald (ms, 1991) include five samples also from the West Branch, and 33 from the Spider Lake Volcanics in the Munsungun Anticlinorium. In the following text, all samples from the Ripogenus Gorge and immediate surrounding areas in the Chesuncook Dome (for example, Fat Man's Woe and Frost Pond) are collectively referred to as the "West Branch suites" (WB). Fitzgerald subdivided the Spider Lake basalts into two suites, based on the uniformity of their compositions: type I basalts (28 samples) show relatively uniform compositions, while type II basalts (5 samples) are more heterogeneous. Ten XRF whole rock analyses come from Gregg and Reusch (2007; two of which were also analyzed using ICP-MS) from the Fish Pond volcanics (FPV) associated with The Forks Formation in the Lobster Mountain Anticlinorium (Sv of Burroughs and Marvinney, 1981). Seven new samples were collected from the Flagstaff Lake Igneous Complex

Table 1

Major and trace element chemical composition of the West Branch Volcanics from Ripogenus Gorge area

Sample:	FPV-01-02	DA	WB-02-21	FW-02-21	RG-02-21	CSK/P-001B
SiO_2	49.42	55.37	50.25	53.88	52.01	54.99
Al_2O_3	16.28	14.97	15.53	14.02	13.92	16.47
TiO_2	2.101	1.93	2.473	3.22	3.32	1.531
FeOT	10.93	9.57	12.35	9.72	12.53	8.75
MnO	0.219	0.142	0.29	0.28	0.239	0.162
CaO	9.68	7.98	7.78	8.7	6.23	6.35
MgO	6.99	5.02	6.43	3.59	5.24	5.26
K_2O	0.44	1.11	0.94	0.68	0.65	0.81
Na_2O	3.67	3.63	3.56	5.44	5.16	5.44
P_2O_5	0.265	0.285	0.415	0.469	0.69	0.237
Ni	32	30	33	12	12	42
Cr	207	111	113	38	27	92
V	320	256	283	380	348	180
Ga	19	21	27	17	21	22
Cu	65	51	52	14	17	34
Zn	91	70	121	94	114	72
La	11.53	23.06	24.61	21.53	27.54	31.69
Ce	26.83	50.74	54.84	48.11	61.04	67.55
Pr	3.72	6.4	7.32	6.29	7.89	8.12
Nd	18.32	28.75	33.05	28.56	36.2	34.83
Sm	5.63	8.06	9.14	8.3	10.19	9.38
Eu	2.01	2.15	3.04	2.52	3.21	2.07
Gd	6.54	8.64	10.05	9.18	10.96	9.64
Tb	1.15	1.55	1.72	1.59	1.92	1.77
Dy	7.24	9.88	10.69	9.96	11.84	11.28
Ho	1.5	2.04	2.21	2.04	2.41	2.39
Er	4	5.62	5.96	5.55	6.49	6.6
Tm	0.57	0.82	0.84	0.78	0.92	0.98
Yb	3.47	5.16	5.11	4.88	5.55	6.27
Lu	0.52	0.79	0.78	0.75	0.87	0.98
Ba	239	181	450	231	211	235
Th	1.07	5.35	3.95	3.56	3.35	9.99
Nb	5.72	9.78	10.49	9.88	11.87	13.64
Y	39.15	54	57.25	52.31	62.59	63.98
Hf	3.96	8	6.95	6.67	7.61	10.87
Ta	0.39	0.69	0.73	0.71	0.82	0.97
U	0.26	1.25	0.91	0.91	0.83	2.24
Pb	2.22	3.32	6.08	2.64	4.48	6.51
Rb	7.4	21.9	22.7	9.2	8	12.9
Cs	0.27	0.53	0.72	0.17	0.4	0.29
Sr	270	211	422	153	169	350
Sc	50.5	37.2	41.5	40.7	40	26.9
Zr	151	327	274	268	322	424
Zr/Y	3.86	6.06	4.79	5.12	5.14	6.63
Ti/Y	321.72	214.27	258.96	369.03	318.00	143.46
Nb/Y	0.15	0.18	0.18	0.19	0.19	0.21
Y/Nb	6.84	5.52	5.46	5.29	5.27	4.69

Table 1
(continued)

Sample:	CSK/P-003	RP-2	RP-3	RP-4	RP-5	RP-9
SiO_2	54.61	50.66	51.1	56.98	53.77	57.07
Al_2O_3	16.1	13.58	13.73	14.39	14.76	13.7
TiO_2	1.501	3.28	3.18	1.78	1.91	0.78
FeOT	8.35	13.42	13.68	8.74	10.49	6.43
MnO	0.134	0.23	0.23	0.14	0.15	0.11
CaO	7	7.68	6.48	7	7.93	6.46
MgO	5.94	4.34	4.06	4.08	5.29	8.07
K_2O	0.86	0.64	0.91	0.67	1.06	3.22
Na_2O	5.32	5.33	5.57	6.34	3.95	3.26
P_2O_5	0.187	0.67	0.72	0.27	0.28	0.37
Ni	30	15	11	35	38	141
Cr	126	23.37	14.56	105.73	122.14	469.78
V	227	389	360	248	254	142
Ga	17	24	21	17	18	15
Cu	48	1	12	32	34	33
Zn	80	110	123	66	91	68
La	11.65	27.51	30.91	22.77	23.44	48.16
Ce	24.94	66.17	74.22	55.18	56.6	105.82
Pr	3.18	NA	NA	NA	NA	NA
Nd	14.63	39.63	43.64	29.34	31.02	56.12
Sm	4.31	10.03	10.8	7.51	7.95	9.74
Eu	1.5	3.02	3.28	1.95	2.04	2.53
Gd	4.94	NA	NA	NA	NA	NA
Tb	0.87	1.46	1.81	1.11	1.22	0.95
Dy	5.57	NA	NA	NA	NA	NA
Ho	1.14	NA	NA	NA	NA	NA
Er	3.11	NA	NA	NA	NA	NA
Tm	0.45	NA	NA	NA	NA	NA
Yb	2.81	5.61	6.21	5.26	5.44	1.35
Lu	0.43	0.88	0.99	0.8	0.87	0.18
Ba	202	363	268	225	196	850
Th	2.23	3.27	3.71	5.34	5.28	11.22
Nb	4.74	11	14	9	7	7
Y	30.43	52	57	43	46	18
Hf	3.39	8.29	9.05	8.41	8.72	5.98
Ta	0.35	0.88	0.89	0.58	0.79	0.57
U	0.67	0.01	0.01	0.01	0.01	2.66
Pb	3.58	0.01	0.01	0.01	0.01	0.01
Rb	14	7	10	0.01	24	45.49
Cs	0.28	NA	NA	NA	NA	NA
Sr	208	282	205	201	241	990
Sc	40.6	37.08	35.04	30.86	34.11	20.96
Zr	132	355	382	342	349	241
Zr/Y	4.34	6.83	6.70	7.95	7.59	13.39
Ti/Y	295.71	378.15	334.46	248.17	248.92	259.78
Nb/Y	0.16	0.21	0.25	0.21	0.15	0.39
Y/Nb	6.42	4.73	4.07	4.78	6.57	2.57

Samples listed are from this study, except those starting with RP, taken from Fitzgerald (1991). Total iron reported as FeOT. NA = not analyzed. BD = below detection limit.

(FL) by M. Dorais and his students and were analyzed using XRF and ICP-MS methods. Sampling in the Flagstaff Lake Igneous Complex was restricted to the main southwestern gabbroic body outcropping between Stratton and Rangeley, Maine along Highway 16. Although this portion of the complex has been previously mapped as gabbro, the vast majority is quartz diorite to tonalite in composition. The tonalite is a metaluminous, hornblende-bearing rock, distinct from the garnet-bearing tonalite that forms a separate map unit (see Appendix 1 for analytical methods used for the Fish Pond Volcanics and Flagstaff Lake gabbros). Fitzgerald (ms, 1991) obtained trace element data using XRF and instrumental neutron activation analysis (INAA) and details of the analysis procedures are given in that report.

All of the samples compiled for this study, including the gabbros, and used in the normalized diagrams and discrimination plots, fall within the basalt or basalt-andesite/andesite fields of the Zr/Ti versus Nb/Y rock classification diagram (fig. 6) of Winchester and Floyd (1977). They have alkali element (Na_2+K_2O) concentrations of 1.92 to 7.26 percent (tables 1, 2, 3, and 4). The Ripogenus Gorge samples have silica contents that range from 49.42 to 57.07 percent and are more siliceous than the Spider Lake basalts that range from 44.34 to 52.99 percent.

Samples analyzed for this study are not visibly deformed (other than by large-scale open folding) by Acadian regional orogenic processes. However, they have experienced low greenschist-grade metamorphism, raising the issue of major element mobility. Therefore our conclusions concerning tectonic environment of extrusion and magma source, are based on immobile trace and rare earth element abundances in these rocks. Further, some rocks observed in the Ripogenus Gorge area contain silicic inclusions that we interpret to be evidence of assimilation of sialic crust, similar to the conclusions reached by Fitzgerald (ms, 1991) and Hon and others (1992). This is supported by higher silica contents and anomalous thorium enrichment seen in several of the discrimination plots used below. Because thorium enrichment is also commonly used to indicate supra-subduction zone settings (for example, Th/Yb-Ta/Yb discrimination plot of Pearce, 1982), we have included an upper continental crustal composition in our thorium-based plots to aid in discrimination between these two interpretations. Due to the absence of direct geochemical analyses of the underlying basement we have used the average continental crust composition of McLennan (2001).

Normalized Rare Earth Element and Multi-Element Diagrams

Chondrite-normalized diagrams of rare earth elements (REEs) are given in figure 7. All samples plotted show a strong negative slope resulting from enrichment of the incompatible light rare earth elements (LREEs). Although all samples show similar negative trends, there are some differences: the type I Spider Lake volcanics of Fitzgerald (ms, 1991; subsequently referred to as SLV-I) are generally less enriched than those of the type II Spider Lake Volcanics (SLV-II), WB, FPV, and FL. Additionally, the SLV-II and WB suites show significantly more scatter than SLV-I, particularly from La to Nd.

Spider diagrams of selected trace elements, normalized to mid-ocean ridge basalts are given in figure 8. They show strong enrichment in Th, La, and Ce with concomitant depletion in the high field strength elements Ta and Nb, although Ta and Nb are still enriched relative to MORB and Y and Yb. Also, high field strength elements (Ta, Nb) show positive anomalies relative to MORB and a negative slope illustrated by relatively high Ti/Y and Zr/Y ratios. Similar to the chondrite-normalized diagram, there is significant scatter in the incompatible trace elements (Th, Ta, Nb, La, and Ce) of the SLV-II and WB suites.

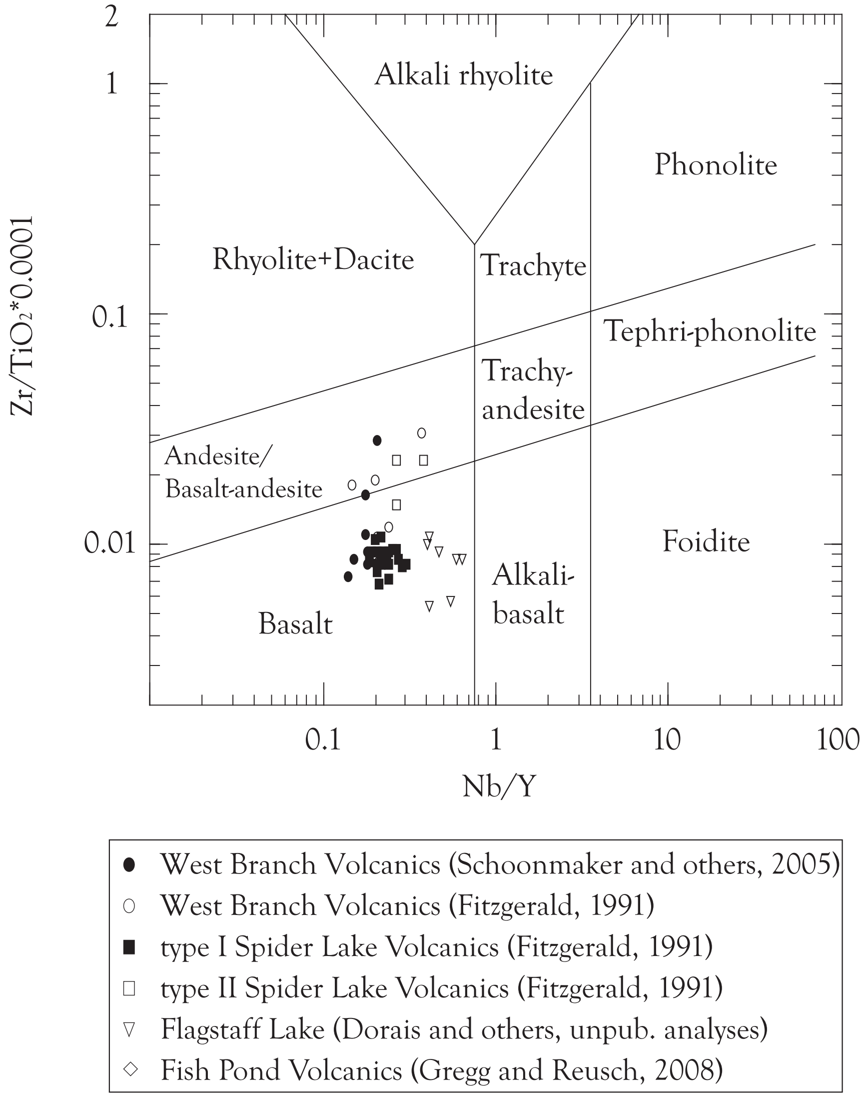

Fig. 6. Rock classification diagram of Winchester and Floyd (1977) using Zr/Ti vs. Nb/Y.

Tectonic Discrimination Diagrams Using Trace Elements

Several tectonic discrimination diagrams (figs. 9, 10, 11, 12, 13, 14, and 15) that use immobile trace elements are included to constrain the environment of the late Silurian and early Devonian volcanism of northern Maine.

The Ti-Zr-Y diagram (fig. 9) of Pearce and Cann (1973) is often used to identify the mantle source of mafic volcanics, although continental tholeiites cannot be discriminated from volcanic arc basalts and MORB using this diagram (Holm, 1982). All samples with measurable Nb have Y/Nb ratios of 2.5 or greater. With one nearby exception, all of SLV-I and FL samples plot in the "within-plate" field (WPB). In contrast, SLV-II and the WB suites are scattered along a linear trend that appears to originate near the locus of the SLV-I group, approximately at the boundary between

TABLE 2

Major and trace elements of the Spider Lake Volcanics (from Fitzgerald, 1991)

Sample:	SP-4	SP-7	SP-11A	SP-11B	SP-14	SP-16	SP-17	SP-20	SP-21	SP-22	SP-23
SiO_2	49.57	49.03	51.49	51.33	49.08	50.34	50.63	47.91	48.5	45.97	52.99
Al_2O_3	17.43	17.17	14.25	14.97	15.53	16.32	14.43	16.32	16.37	17.34	15.46
TiO_2	2.03	1.73	2.09	2.1	2.18	1.89	2.02	1.76	1.91	2.14	1.94
FeOT	10.95	10.89	14.63	12.58	12.43	10.78	12.6	10.87	11.71	11.01	12.66
MnO	0.16	0.16	0.14	0.15	0.2	0.11	0.14	0.14	0.17	0.17	0.11
CaO	6.83	10.33	6	6.33	8.67	6.69	10.03	12.31	9.04	10.86	8.04
MgO	7.48	7.22	7.18	8.01	6.76	7.63	5.56	6.26	7.87	7.21	4.06
K_2O	0.73	0.48	0.13	0.15	1.11	0.94	0.48	0.32	0.24	0.83	0.38
Na_2O	4.78	2.48	4.08	4.44	3.37	4.28	3.7	3.06	4	4.41	4.18
P_2O_5	0.32	0.25	0.32	0.33	0.31	0.29	0.29	0.24	0.25	0.31	0.28
Ni	106	107	111	116	72	111	66	101	112	103	58
Cr	221.74	186.07	194.57	199.8	168.42	144.36	173.16	203.95	192.3	148.86	145.99
V	275	227	279	270	299	271	279	239	242	309	286
Ga	16	19	18	19	17	20	18	19	17	14	19
Cu	38	41	17	30	22	14	57	35	44	30	0
Zn	96	85	101	105	103	81	86	80	94	86	91
La	11.25	11.46	13.84	12.45	13.53	12.36	11.9	8.62	10.65	11.67	13.43
Ce	27.61	26.78	32.49	31.64	32.88	31.11	29.77	26.73	26.2	27.15	32.27
Pr	NA	NA	NA	NA	NA	NA	NA	NA	NA	NA	NA
Nd	18.67	19.66	19.63	20.39	21.48	17.63	19.36	17.68	17.17	17.54	21.94
Sm	4.99	4.66	5.17	5.4	5.49	4.66	5.1	4.65	4.59	4.64	5.09
Eu	1.69	1.65	1.69	1.57	1.92	1.67	1.77	1.69	1.69	1.54	1.68
Gd	NA	NA	NA	NA	NA	NA	NA	NA	NA	NA	NA
Tb	0.68	0.66	0.7	0.73	0.72	0.7	0.7	0.63	0.61	0.64	0.74
Dy	NA	NA	NA	NA	NA	NA	NA	NA	NA	NA	NA
Ho	NA	NA	NA	NA	NA	NA	NA	NA	NA	NA	NA
Er	NA	NA	NA	NA	NA	NA	NA	NA	NA	NA	NA
Tm	NA	NA	NA	NA	NA	NA	NA	NA	NA	NA	NA
Yb	2.96	2.82	3.06	3.33	3.41	2.89	3.18	2.9	2.81	2.79	3.11
Lu	0.45	0.44	0.45	0.49	0.56	0.45	0.47	0.46	0.38	0.45	0.53
Ba	441	162	32	38	703	241	82	112	74	65	55
Th	0.53	0.65	0.95	0.6	1.49	1.03	0.88	0.81	0.68	1.25	1.49
Nb	7	6	7	8	6	8	6	7	8	6	7
Y	31	26	30	32	31	28	27	27	27	24	28
Hf	3.98	3.67	4.27	4.41	4.63	3.76	4.08	3.76	3.55	3.69	4.38
Ta	0.45	0.32	0.39	0.64	0.33	0.59	0.32	0.25	0.25	0.37	0.38
U	NA	NA	NA	NA	NA	NA	NA	NA	NA	NA	NA
Pb	NA	NA	NA	NA	NA	NA	NA	NA	NA	NA	NA
Rb	7	BD	BD	BD	BD	14	BD	BD	BD	17.51	BD
Cs	NA	NA	NA	NA	NA	NA	NA	NA	NA	NA	NA
Sr	540	440	92	83	270	350	240	307	234	212	289
Sc	33.48	30.92	30.78	30.51	36.76	29.57	36.08	32.67	32.71	30.35	32.81
Zr	180	162	175	173	185	162	168	168	154	151	180
Zr/Y	5.81	6.23	5.83	5.41	5.97	5.79	6.22	6.22	5.70	6.29	6.43
Ti/Y	392.58	398.90	417.65	393.42	421.58	404.66	448.51	390.79	424.09	534.55	415.37
Nb/Y	0.23	0.23	0.23	0.25	0.19	0.29	0.22	0.26	0.30	0.25	0.25
Y/Nb	4.43	4.33	4.29	4.00	5.17	3.50	4.50	3.86	3.38	4.00	4.00

Table 2

(continued)

Sample:	SP-24	SP-25	SP-26	SP-27	SP-28	SP-29	SP-30	SP-32	SP-33	SP-38	SP-39
SiO_2	48.45	48.52	46.84	48.81	49.44	49.61	47.74	50.96	52.53	52.59	49.38
Al_2O_3	16.98	17.36	16.77	16.15	15.11	16.98	17.02	16.18	15.24	15.71	17.13
TiO_2	2.09	1.78	1.75	2.21	2.69	1.75	1.84	1.95	2.85	2.17	1.61
FeOT	11.6	10.77	10.91	11.65	12.95	10.81	10.83	10.76	11.86	11.01	10.74
MnO	0.19	0.13	0.19	0.18	0.18	0.15	0.21	0.13	0.22	0.21	0.18
CaO	7.53	8.34	9.21	8.02	9.4	9.09	9.99	9.52	7.67	7.04	7
MgO	7.64	8.25	9.45	7.83	6.27	7.84	8.06	6.58	4.37	5.25	8.88
K_2O	1.31	1.24	0.71	0.96	0.36	0.86	0.52	0.62	0.79	1.78	0.29
Na_2O	4.02	4.65	4.14	4.09	3.56	2.8	3.56	3.07	4.11	5.19	4.92
P_2O_5	0.32	0.27	0.27	0.31	0.44	0.24	0.26	0.26	0.43	0.38	0.2
Ni	118	114	158	66	49	109	96	97	21	49	130
Cr	170.44	221.38	292.34	185.79	99.16	189.63	191.59	201.82	186.87	154.73	230.74
V	275	230	219	294	349	226	253	264	360	290	236
Ga	19	20	17	19	22	14	18	17	27	18	16
Cu	28	0	43	48	21	12	31	48	31	33	43
Zn	97	89	90	107	131	86	97	92	119	95	88
La	11.59	11.12	10.1	14.2	18.78	10.41	11.18	11.57	23.13	17.86	7.44
Ce	28.91	27.15	25.47	34.64	46.48	25.85	26.88	28	55.45	42.36	18.05
Pr	NA	NA	NA	NA	NA	NA	NA	NA	NA	NA	NA
Nd	17.31	16.89	17.42	22.87	29.12	17.5	17.33	19.29	33.64	25.39	12.85
Sm	5.02	4.46	4.37	5.69	7.49	4.45	4.66	4.86	8.28	6.33	3.76
Eu	1.76	1.55	1.46	1.94	2.35	1.54	1.66	1.65	2.56	2	1.3
Gd	NA	NA	NA	NA	NA	NA	NA	NA	NA	NA	NA
Tb	0.68	0.59	0.61	0.81	1.02	0.61	0.52	0.65	1.2	0.85	0.5
Dy	NA	NA	NA	NA	NA	NA	NA	NA	NA	NA	NA
Ho	NA	NA	NA	NA	NA	NA	NA	NA	NA	NA	NA
Er	NA	NA	NA	NA	NA	NA	NA	NA	NA	NA	NA
Tm	NA	NA	NA	NA	NA	NA	NA	NA	NA	NA	NA
Yb	2.84	2.74	2.76	3.6	4.84	2.7	2.78	2.97	4.9	3.73	2.32
Lu	0.4	0.41	0.43	0.48	0.72	0.38	0.4	0.45	0.79	0.58	0.34
Ba	1037	307	144	201	123	201	148	222	376	371	62
Th	0.6	0.59	0.6	1.29	2.07	0.88	0.73	0.85	3.57	1.7	0.47
Nb	9	6	BD	8	8	7	BD	BD	9	9	BD
Y	29	28	28	33	41	27	25	27	43	40	23
Hf	3.92	3.82	3.32	4.75	6.58	3.79	3.88	3.94	7.4	5.5	3
Ta	0.4	0.31	0.31	0.48	0.47	0.26	0.26	0.32	0.67	0.54	0.26
U	NA	NA	NA	NA	NA	NA	NA	NA	NA	NA	NA
Pb	NA	NA	NA	NA	NA	NA	NA	NA	NA	NA	NA
Rb	23	28	9	12	BD	22.62	7	6	11	54.14	BD
Cs	NA	NA	NA	NA	NA	NA	NA	NA	NA	NA	NA
Sr	358	397	328	167	201	380	270	346	300	373	407
Sc	32.56	31.62	32.47	38.62	36.72	30.54	30.82	32.65	33.19	35.98	23.77
Zr	172	167	140	187	251	166	157	165	298	235	123
Zr/Y	5.93	5.96	5.00	5.67	6.12	6.15	6.28	6.11	6.93	5.88	5.35
Ti/Y	432.05	381.11	374.69	401.48	393.33	388.56	441.23	432.97	397.34	325.23	419.65
Nb/Y	0.31	0.21	BD	0.24	0.20	0.26	BD	BD	0.21	0.23	BD
Y/Nb	3.22	4.67	BD	4.13	5.13	3.86	BD	BD	4.78	4.44	BD

Table 2

(continued)

Sample:	SP-41	SP-42	SP-44	SP-45	SP-46	SP-50	SP-35	SP-36	SP-37	SP-47	SP-53
SiO_2	52.28	50.24	47.88	48.4	49.15	51.06	50.71	50.97	50.97	44.34	53.1
Al_2O_3	14.73	15.33	16.2	17.45	16.9	16.87	15.57	17.5	18.24	15.22	18.17
TiO_2	2.47	2.03	2.11	1.6	2.07	1.77	1.33	1.37	1.54	1.35	1.29
FeOT	11.58	12.01	11.35	10.02	11.38	9.61	8.36	8.39	9.87	9.79	9.13
MnO	0.18	0.17	0.19	0.2	0.17	0.13	0.2	0.11	0.11	0.12	0.11
CaO	7.02	7.11	10.22	9.34	6.07	8.35	14.27	10.15	8.51	20.15	7.79
MgO	6.07	7.76	7.06	8.28	8.77	7.33	3.04	4.49	4.66	2.16	2.41
K_2O	0.13	1.04	0.62	1.28	1.07	1.39	0.4	0.41	1.09	1.6	0.14
Na_2O	5.38	4.66	2.94	3.01	4.38	3.04	6.56	4.92	4.98	5.66	7.02
P_2O_5	0.41	0.28	0.29	0.13	0.31	0.27	0.23	0.49	0.4	0.22	0.45
Ni	37	87	79	153	126	107	112	121	161	74	86
Cr	104.38	164.37	120.62	275.41	179.41	201.04	28.46	131.63	299.86	153.53	191.75
V	342	284	266	235	281	222	139	151	191	137	104
Ga	20	15	18	17	20	17	14	18	18	11	17
Cu	245	79	34	68	0	21	BD	47	102	32	BD
Zn	112	98	95	75	104	82	76	106	80	56	74
La	17.31	13.34	49.1	4.75	11.32	11.66	13.84	34.15	23.88	5.52	34.45
Ce	41.05	31.55	26.57	13.2	27.91	27.99	30.78	74.03	51.82	13.01	70.3
Pr	NA	NA	NA	NA	NA	NA	NA	NA	NA	NA	NA
Nd	26.72	18.83	18.7	11.16	19.55	16.62	16.76	32.25	26.73	9.94	31.71
Sm	6.64	5.07	5.01	3.55	4.84	4.56	4.01	6.57	5.7	2.69	5.93
Eu	2.35	1.76	1.59	1.29	1.65	1.64	1.3	2.01	1.77	1.07	1.69
Gd	NA	NA	NA	NA	NA	NA	NA	NA	NA	NA	NA
Tb	0.92	0.58	0.57	0.5	0.59	0.54	0.52	0.8	0.7	0.4	0.77
Dy	NA	NA	NA	NA	NA	NA	NA	NA	NA	NA	NA
Ho	NA	NA	NA	NA	NA	NA	NA	NA	NA	NA	NA
Er	NA	NA	NA	NA	NA	NA	NA	NA	NA	NA	NA
Tm	NA	NA	NA	NA	NA	NA	NA	NA	NA	NA	NA
Yb	4.14	2.8	2.89	2.77	3.09	2.6	2.09	3.01	2.83	1.8	2.89
Lu	0.69	0.43	0.44	0.4	0.45	0.4	0.36	0.48	0.43	0.28	0.44
Ba	36	339	143	745	465	272	80	463	456	383	75
Th	1.79	0.62	0.79	1.58	0.93	1.07	1.37	4.46	2.24	0.4	6.03
Nb	9	6	BD	5	6	8	BD	8	9	BD	10
Y	37	28	27	23	28	29	18	29	33	21	25
Hf	5.4	4.1	3.81	2.96	3.94	3.95	3.37	6.88	5.29	1.99	6.8
Ta	0.41	0.45	0.39	0.15	0.3	0.4	0.18	0.75	0.66	0.23	0.77
U	NA	NA	NA	NA	NA	NA	NA	NA	NA	NA	NA
Pb	NA	NA	NA	NA	NA	NA	NA	NA	NA	NA	NA
Rb	6	12	6	31	12	29.74	9	6	15	36	BD
Cs	NA	NA	NA	NA	NA	NA	NA	NA	NA	NA	NA
Sr	276	215	414	226	430	253	231	208	142	253	255
Sc	38.62	34.4	32.69	38.51	32.83	30.22	33.69	22.98	26.26	24.65	22.16
Zr	217	169	163	107	158	168	136	316	229	75	303
Zr/Y	5.86	6.04	6.04	4.65	5.64	5.79	7.56	10.90	6.94	3.57	12.12
Ti/Y	400.21	434.64	468.50	417.04	443.20	365.90	442.96	283.21	279.77	385.39	309.34
Nb/Y	0.24	0.21	BD	0.22	0.21	0.28	BD	0.28	0.27	BD	0.40
Y/Nb	4.11	4.67	BD	4.60	4.67	3.63	BD	3.63	3.67	BD	2.50

TABLE 3

Major and trace elements of the Flagstaff Lake complex

Sample:	FL-5	FL-6	FL-7	FL-9	FL-10	FL-11	FL-12
SiO_2	46.39	53.74	56.25	52.19	50.55	52.04	54.29
Al_2O_3	15.31	14.23	14.14	15.44	16.49	16.13	16.68
TiO_2	3.06	2.9	2.32	2.49	2.09	1.9	2.04
FeOT	14.65	11.68	10.93	11.87	10.46	9.91	9.67
MnO	0.16	0.15	0.13	0.17	0.14	0.12	0.21
CaO	7.9	6.62	6.28	8.03	8.42	7.67	6.63
MgO	6.13	3.53	3.02	4.18	6.14	5.89	2.96
K_2O	1.22	1.72	1.99	1.46	1.22	1.47	1.8
Na_2O	2.48	2.9	2.86	3.12	2.80	2.87	3.66
P_2O_5	0.4	0.57	0.87	0.48	0.32	0.31	0.51
Ni	63	8	5	13	72	76	7
Cr	48	3	1	45	137	126	8
V	446	322	246	324	271	235	253
Ga	21.9	26.3	24	22.4	20.7	20.2	22.8
Cu	56	30	23	29	54	45	22
Zn	130	138	123	111	88	86	108
La	14.6	28.7	25.8	20.8	15.7	17.1	24.7
Ce	34.9	66.4	63.7	50.9	39	42.4	66.8
Pr	5.32	9.35	10.15	7.76	6.06	6.41	10.55
Nd	23.4	40.2	46.3	34.1	27.3	28.2	48.1
Sm	5.65	9.07	11.65	8.01	6.45	6.73	11.75
Eu	1.89	2.82	2.8	2.3	1.95	1.79	2.67
Gd	5.9	10.05	12.35	8.8	6.94	7.01	12.1
Tb	0.89	1.44	1.87	1.27	1.06	1.06	1.76
Dy	5.06	8.51	10.55	7.56	6.15	6.26	10.05
Ho	1	1.66	1.95	1.51	1.27	1.28	1.93
Er	2.81	4.55	5.18	4.14	3.52	3.47	5.23
Tm	0.4	0.63	0.66	0.61	0.5	0.5	0.73
Yb	2.38	3.73	3.68	3.45	3.09	2.92	4.43
Lu	0.38	0.59	0.54	0.55	0.46	0.45	0.66
Ba	127.5	334	306	232	133.5	226	332
Th	3.07	3.07	3.39	4	3.03	3.05	3.02
Nb	9	14	14	13	10	10	24
Y	22.1	35.9	42	32.7	27.4	27.7	42.1
Hf	4.6	7.1	3.8	6.6	5.8	5.7	5
Ta	0.9	1.5	1.1	1.1	0.8	0.8	1.5
U	0.82	1.24	1.15	1.28	0.9	1.48	0.97
Pb	34	10	10	9	7	12	11
Rb	59.4	63.5	72	47.4	52.7	53.5	55.1
Cs	7.06	2.04	2.18	2.23	1.46	1.43	1.71
Sr	352	305	294	295	352	298	300
Sc	NA	NA	NA	NA	NA	NA	NA
Zr	173	253	126	234	211	204	178
Zr/Y	7.83	7.05	3.00	7.16	7.70	7.36	4.23
Ti/Y	830.08	484.28	331.01	456.50	456.85	411.21	290.49
Nb/Y	0.56	0.62	0.43	0.48	0.42	0.42	0.66
Y/Nb	1.78	1.62	2.32	2.08	2.38	2.37	1.52

the "within-plate" field and the "low potassium tholeiite" and "calc-alkaline" overlap fields (OFB). The trend shows increasing Zr enrichment and/or depletion of Ti concentrations (relative to Y), extending away from this locus through the "calc-alkaline" field (CAB) towards the average composition of continental crust. All samples however, plot in the fields (OFB, CAB, and WPB) identified as also representing within-plate continental tholeiites by Holm (1982). It should be noted that Zr/Y ratios of the WB suites appear to vary systematically from low Zr/Y in samples from

Table 4

Major and trace elements of the Fish Pond Volcanics from the Lobster Mountain Anticlinorium

Sample:	SUVM 5	SUVM 6	SUVM 7	SUVM 8	SUVM 9	SUVM 10	SUVM 11	SUVM 12b	SUVM 4	SUVM 14
SiO_2	46.97	55.68	49.42	49.74	49.18	46.36	48.99	48.34	50.68	51.77
Al_2O_3	14.34	12.94	14.21	13.01	17.27	15.07	13.66	12.63	12.98	13.05
TiO_2	4.359	3.763	4.035	3.892	1.639	4.191	4.127	3.666	3.574	3.65
FeOT	15.78	11.14	15.32	14.59	10.63	15.77	15.47	13.18	14.59	13.42
MnO	0.236	0.187	0.258	0.244	0.163	0.233	0.26	0.278	0.263	0.217
CaO	5.73	6.76	5.88	7.14	8.32	5.78	6.66	7.8	7.34	6.48
MgO	6.06	3.13	5.19	4.57	6.88	5.27	5.48	4.43	5.35	3.9
K_2O	2.49	0.38	0.39	0.64	0.68	0.25	0.54	0.74	1.13	0.47
Na_2O	2.62	6.47	5.05	4.6	3.38	6.25	5.28	4.29	4.17	5.06
P_2O_5	0.742	0.831	0.775	0.739	0.216	0.793	0.789	0.717	0.824	0.69
Ni	NA	NA	NA	NA	NA	NA	NA	NA	NA	NA
Cr	53	45	45	47	71	52	46	37	38	45
V	NA	NA	NA	NA	NA	NA	NA	NA	NA	NA
Ga	NA	NA	NA	NA	NA	NA	NA	NA	NA	NA
Cu	NA	NA	NA	NA	NA	NA	NA	NA	NA	NA
Zn	142	76	133	125	71	147	141	122	117	83
La	NA	NA	NA	NA	NA	NA	NA	NA	NA	NA
Ce	NA	NA	NA	NA	NA	NA	NA	NA	NA	NA
Pr	NA	NA	NA	NA	NA	NA	NA	NA	NA	NA
Nd	NA	NA	NA	NA	NA	NA	NA	NA	NA	NA
Sm	NA	NA	NA	NA	NA	NA	NA	NA	NA	NA
Eu	NA	NA	NA	NA	NA	NA	NA	NA	NA	NA
Gd	NA	NA	NA	NA	NA	NA	NA	NA	NA	NA
Tb	NA	NA	NA	NA	NA	NA	NA	NA	NA	NA
Dy	NA	NA	NA	NA	NA	NA	NA	NA	NA	NA
Ho	NA	NA	NA	NA	NA	NA	NA	NA	NA	NA
Er	NA	NA	NA	NA	NA	NA	NA	NA	NA	NA
Tm	NA	NA	NA	NA	NA	NA	NA	NA	NA	NA
Yb	NA	NA	NA	NA	NA	NA	NA	NA	NA	NA
Lu	NA	NA	NA	NA	NA	NA	NA	NA	NA	NA
Ba	572	BD	BD	27	175	BD	BD	102	51	BD
Th	NA	NA	NA	NA	NA	NA	NA	NA	NA	NA
Nb	27	20	23	22	BD	23	23	23	23	21
Y	60	52	54	54	28	52	53	51	57	50
Hf	NA	NA	NA	NA	NA	NA	NA	NA	NA	NA
Ta	NA	NA	NA	NA	NA	NA	NA	NA	NA	NA
U	NA	NA	NA	NA	NA	NA	NA	NA	NA	NA
Pb	NA	NA	NA	NA	NA	NA	NA	NA	NA	NA
Rb	55	8	8	23	20	8	10	22	25	16
Cs	NA	NA	NA	NA	NA	NA	NA	NA	NA	NA
Sr	496	226	309	286	414	250	312	649	493	294
Sc	NA	NA	NA	NA	NA	NA	NA	NA	NA	NA
Zr	398	324	361	356	190	351	352	356	317	335
Zr/Y	6.63	6.23	6.69	6.59	6.79	6.75	6.64	6.98	5.56	6.70
Ti/Y	435.54	433.83	447.96	432.08	350.92	483.17	466.82	430.93	375.90	437.64
Nb/Y	0.45	0.38	0.43	0.41	BD	0.44	0.43	0.45	0.40	0.42
Y/Nb	2.22	2.60	2.35	2.45	BD	2.26	2.30	2.22	2.48	2.38

Samples listed are from Gregg and Reusch (2007). Total iron reported as FeOT. NA = not analyzed. BD = below detection limit.

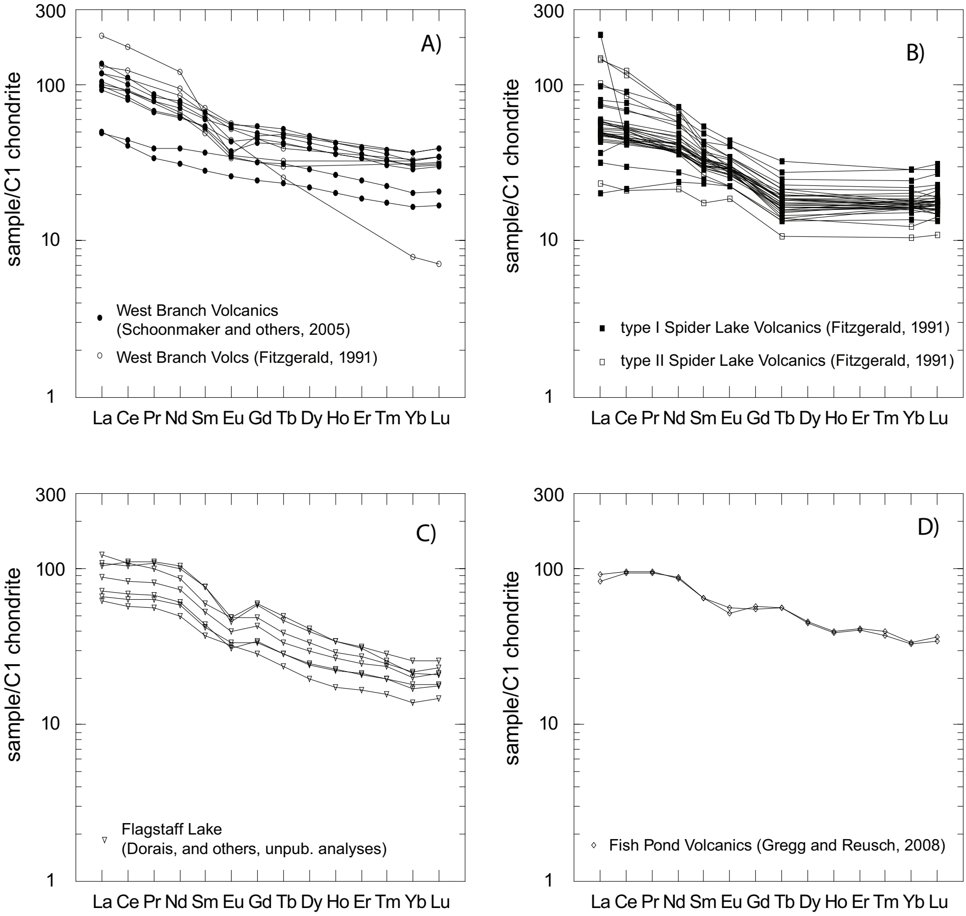

Fig. 7. C1-chondrite normalized diagrams of rare earth elements (REE). Normalization values from Sun and McDonough (1989).

Schoonmaker and others (2005) to high Zr/Y in West Branch samples from Fitzgerald (ms, 1991) suggesting an analytical bias in Zr and/or Y concentrations, in one, or both of the suites. This is also evident in the Nb-Zr-Y diagram (below).

The Th-Ta-Hf diagram (fig. 10) of Wood and others (1979) and Wood (1980) can be used to identify volcanic arc settings, identify continental crustal contamination, and determine the mantle source of volcanics. The SLV-I basalts mainly straddle the "N-MORB" field and the "arc tholeiite" subfield of the "destructive plate margin and differentiates" field, with the exception of two samples that plot in the "E-type MORB and tholeiitic within-plate basalts and differentiates" field. Of those that plot in the N-MORB field, all plot in or near the overlap region with the E-MORB and WPT field. The SLV-II basalts and WB suites (with two exceptions) plot in the calc-alkaline subfield of the volcanic arc field.

The Nb-Zr-Y diagram (fig. 11) of Meschede (1986) is also commonly used to discriminate between mantle sources, especially between N-type MORB, E-type MORB, within-plate tholeiites, and within-plate alkaline basalts, by using Nb as a discriminator instead of Ti. However, like the Ti-Zr-Y, it does not uniquely identify supra-subduction

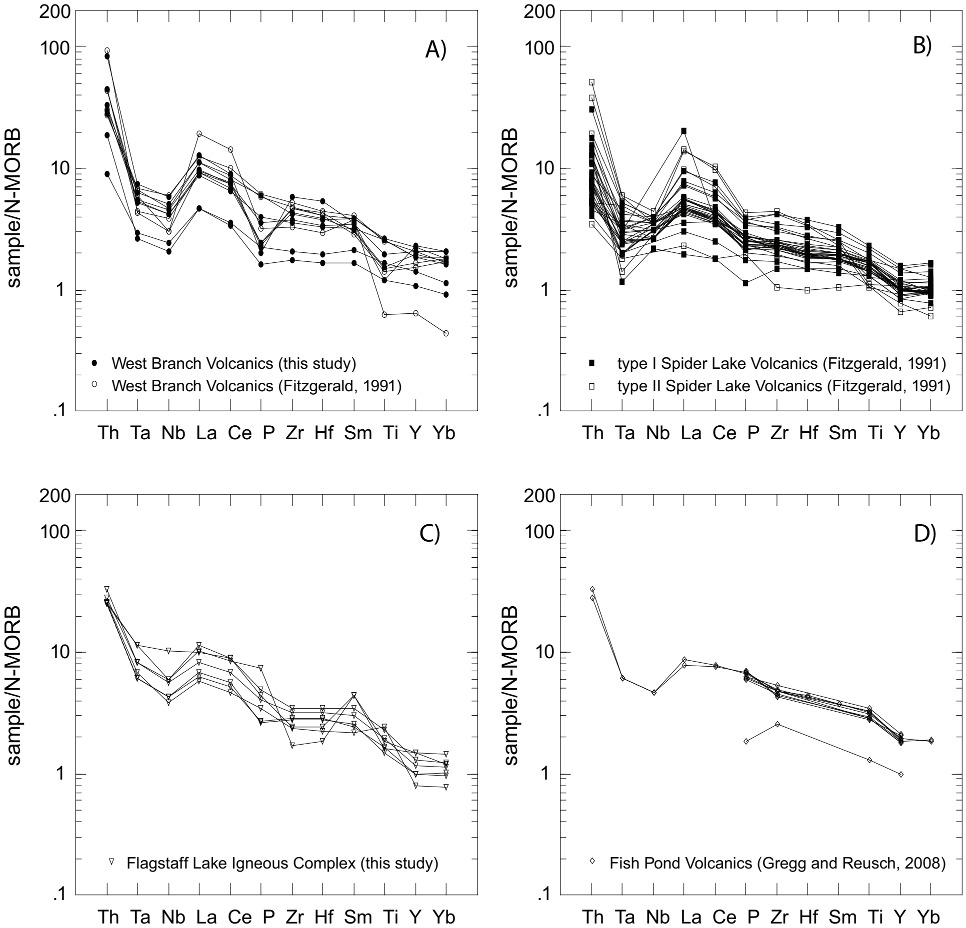

Fig. 8. MORB-normalized diagrams of selected trace elements. Normalization values from Sun and McDonough (1989).

zone settings. The SLV-I basalts plot in a tight pattern in the "within-plate tholeiite" and "volcanic arc basalt" field (C), while the SLV-II basalts, the WB suites, and FL samples plot along a trend of varying Zr and Y ratios across this field; Nb versus Zr or Y concentrations do not appear to be particularly influenced here, while Zr/Y ratios are variable to the extent that several plot outside of the delineated fields.

The Th/Yb-Ta/Yb diagram (fig. 12) of Pearce (1982) has been used to identify supra-subduction zone magmatism, based on the anomalous enrichment of Th relative to Ta in arc magmas. Th-enriched magmas plot above the "mantle array" in progressively enriched "island arc tholeiite" (IAT), "calc-alkaline basalt" (CAB), and "shoshonite" (SHO) fields. Similarly, magmas contaminated with upper continental crust show anomalous Th-enrichment as indicated by the composition of average upper continental crust and assimilation and fractional crystallization vector (AFC) shown in the diagram. The SLV-I basalts are clustered near the mantle array, straddling the IAT and CAB fields, while the SLV-II, WB, and FL suites have higher concentrations of Th relative to Ta and plot almost fully in the CAB field.

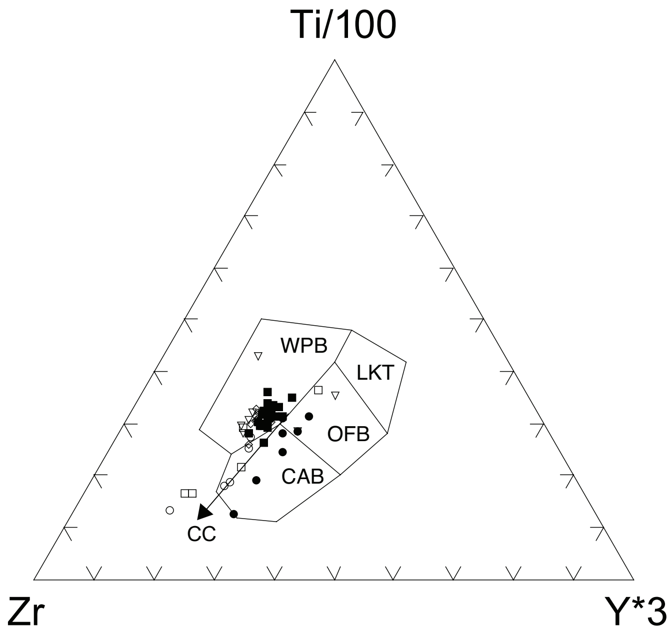

Fig. 9. Ti-Zr-Y diagram of Pearce and Cann (1973). WPB = within plate basalts (oceanic and continental), OFB = ocean floor basalts, LKT = low-K tholeiites, CAB = calc-alkaline basalts. CC = average upper continental crust composition (from McLennan, 2001). See figure 6 for symbol explanation.

The Ti-V diagram (fig. 13) of Shervais (1982) and Cr-Y diagram (fig. 14) of Pearce (1982) both discriminate between arc and non-arc settings without relying on Th enrichment or Ta-Nb depletion. On the Ti-V plot, nearly all samples plot near the divide between alkalic rocks (Ti/V >50) and sub-alkaline rocks. The SLV-II, WB, and FL suites show a wide range of Ti and V absolute abundances, although the SLV-I basalts are relatively uniform in Ti and V abundances.

The Cr-Y diagram (fig. 14) of Pearce (1982) differentiates volcanic arc basalts from within-plate basalts and MORB based on incompatible Y content. As partial melting of mantle increases, compatible Cr is relatively unchanged, but Y concentrations in the melt are diluted and decrease in concentration. Higher degrees of partial melting above subducting slabs may, in part, account for lower Y concentrations in VAB, relative to MORB and within-plate basalts. During subsequent fractional crystallization, Cr concentrations in the melt decrease as it is partitioned into crystallizing mafic phases, while Y remains relatively unchanged. Most samples plot in the overlap field of MORB and WPB fields with some also falling within the VAB field. However, some (mainly Flagstaff Lake and Fish Pond Volcanics) plot outside the MORB field, either exclusively within the VAB or more commonly in the WPB field, or entirely outside the delineated fields (but near WPB).

The Ce/Nb-Th/Nb diagram (fig. 15) of Saunders and others (1988) uses Th and Ce to discriminate between MORB and volcanic arc basalts. Ce is elevated in arc basalts, but not in upper continental crust, relative to MORB, so the arc and crustal contamination vectors diverge significantly. While the SLV-I, SLV-II, and FL suites basalts plot within the backarc basin field (BABB), they form a linear Th-enrichment trend towards the composition of upper continental crust.

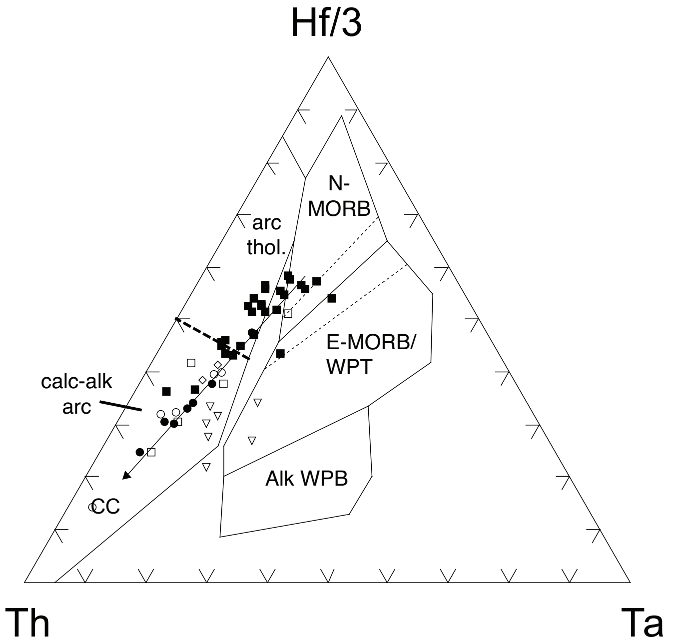

Fig. 10. Th-Hf-Ta diagram of Wood (1980). Calc-Alk Arc = calc-alkaline volcanic arc basalt, Arc Thol. = volcanic arc tholeiite, N-MORB = normal, depleted mid-ocean ridge basalt, E-MORB/WPT = enriched mid-ocean ridge basalt and within-plate tholeiite, Alk WPB = alkaline within-plate basalt. The two arc subfields are collectively referred to as the "destructive margin and differentiates" field, separated by the dashed line. CC = average upper continental crust composition (from McLennan, 2001). See figure 6 for symbol explanation.

Neodymium Isotope Geochemistry

Five West Branch Volcanics were analyzed for neodymium isotopic ratios (table 5); analytical procedures are given in Appendix 1. Initial $^{143}Nd/^{144}Nd$ values and ε_{Nd} values were calculated using a 417 Ma model age, which was assigned based on late Ludlow to early Lockhovian conodonts in the underlying limestones of the Ripogenus Formation. $^{147}Sm/^{144}Nd$ values were calculated using the ratio of Sm and Nd absolute abundances (from table 1) multiplied by a conversion factor of .605.

Initial $^{143}Nd/^{144}Nd$ values range from .512221 to .512297 and are similar to those from mafic volcanic rocks from volcanic arcs and continental flood basalts, and xenoliths of subcontinental lithosphere (Rollinson, 1993; Faure and Mensing, 2005). Resulting ε_{Nd} values fall in a relatively narrow range +2.3 to +3.8, although the suite size is small, and are typical of juvenile mafic rocks.

Discussion

The volcanic rocks analyzed in this study are basalts and basalt-andesites (fig. 6) with positive ε_{Nd} values that indicate they were derived from either a relatively uncontaminated moderately enriched mantle, or from a depleted mantle and subsequently contaminated with a component of continental crust (fig. 16). Their trace element geochemistries do not yield a unique interpretation on tectonic discrimination diagrams, generally displaying characteristics of volcanic arc, continental within-plate tholeiites, backarc basins, and MOR. This is similar to patterns seen in the New Brunswick Tobique Volcanic Belt and Miramichi Highlands where samples plot in

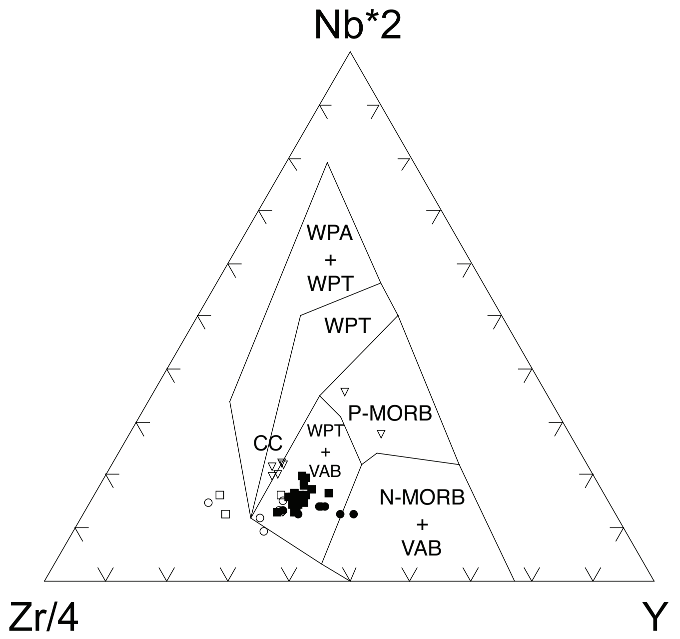

Fig. 11. Nb-Zr-Y diagram of Meschede (1986). WPA = within-plate alkaline basalts, WPT = within-plate tholeiites, P-MORB = plume-influenced mid-ocean ridge basalt, N-MORB = normal, mid-ocean ridge basalt, VAB = volcanic arc basalt. CC = average upper continental crust composition (from McLennan, 2001). See figure 6 for symbol explanation.

both volcanic arc and within-plate fields of discrimination diagrams (for example, Dostal and others, 1989; and fig. 15 of van Staal and others, 2009). Further complicating matters, the chondrite-normalized diagrams (fig. 7) indicate an enriched mantle source while many of the discrimination diagrams display trends that originate from depleted mantle sources, consistent with the positive ε_{Nd} values.

On all geochemical diagrams and plots, SLV-I samples have relatively uniform compositions, while SLV-II, WB, and FL rocks show greater scatter along approximately linear trends at the end of which the SLV-I rocks tend to cluster. On some diagrams (but not all), SLV-I rocks have more primitive compositions, while the SLV-II, WB, and FL rocks are more evolved; SLV-II, WB, FPV, and FL rocks have lower concentrations of MgO, Ni, and Cr, and higher concentrations of SiO_2, Zr, Y, Ti, and P (the major element concentrations may be suspect due to metamorphism, but these trends are noted). Further, the SLV-II, WB, and to a lesser extent the FL rocks appear to have been displaced towards the composition of upper continental crust (CC on diagrams), while SLV-I rocks are less so. Previous workers (Hon and others, 1992; Schoonmaker and others, 1995) have suggested that these rocks may have been affected by assimilation of continental crust material. If true, more evolved suites (SLV-II, WB, FPV, and FL) might have been derived from melts that resided in the upper crust for longer periods of time, assimilating country rock material before eruption, and the more primitive SLV-I rocks erupted rather quickly on the surface, experiencing little assimilation or fractional crystallization. This hypothesis is supported if the ε_{Nd} values are the result of melts derived from an originally depleted mantle source that incorporated some component of granitic continental crust during ascent.

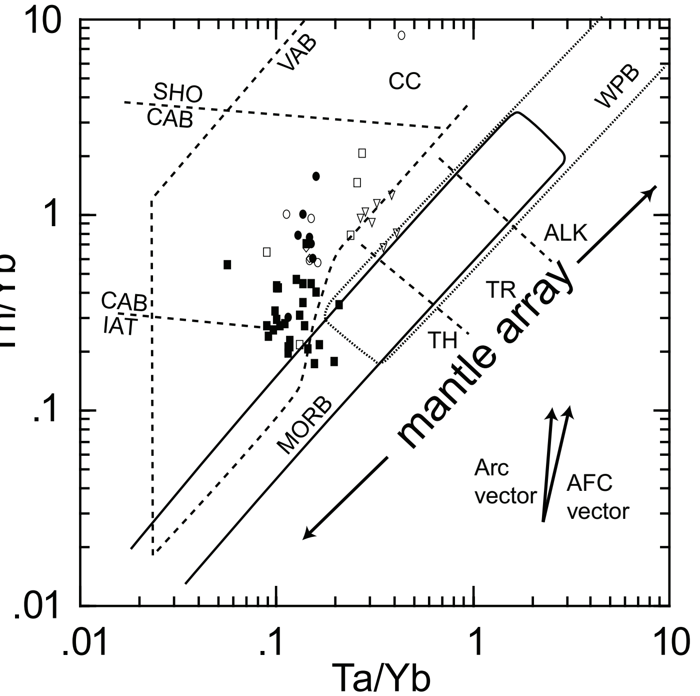

Fig. 12. Th/Yb-Ta/Yb diagram of Pearce (1982). MORB = mid-ocean ridge basalt, WPB = within-plate basalt, TH = tholeiitic basalts, ALK = alkaline basalts, TR = transitional basalts, IAT = island arc tholeiite field, CAB = calc-alkaline basalt field, SHO = shoshinitic basalt field. CC = average upper continental crust composition (from McLennan, 2001). See figure 6 for symbol explanation.

The chondrite-normalized diagrams (fig. 7) are relatively simple and show these rocks are enriched in REE, especially LREE, indicative of an enriched mantle source (for examples, Rollinson, 1993), although this interpretation contrasts with the positive ε_{Nd} values of the WB rocks. The MORB-normalized diagrams (fig. 8) are also problematic; Th and Ce are strongly enriched relative to Ta and Nb. This general pattern is usually identified as an arc signature resulting from supra-subduction zone processes (for example, Pearce and others, 1995). Typical arc patterns show depletion (or only minor enrichment) of Ta and Nb relative to MORB, and Ta and Nb ratios (relative to MORB) are generally similar or less than Y and Yb ratios. For the most part, Ta and Nb are up to about 10 times more enriched than MORB and Ta and Nb ratios are higher than Y and Yb ratios in figure 8. Also, the negative trend seen in the chondrite-normalized diagrams is present from La to Yb in the MORB-normalized diagrams and is characteristic of rocks derived from an enriched source rather than from typical depleted mantle above subduction zones whose overall patterns, while spiky, have flatter trends. The negative trend is illustrated by high Ti/Y and Zr/Y ratios, characteristic of enriched sources.

In the context of surrounding country rock (continental crust overlain by shallow marine sedimentary rocks), at least two possible conclusions may be drawn from these data: 1) the chondrite- and MORB-normalized diagrams indicate a possible continental arc environment, but if so, one that taps a modified or heterogeneous mantle source, possibly an incipient back-arc basin, or 2) a modified mantle was tapped in a non-arc, non-MORB environment (for example, within-plate) and the arc characteris-

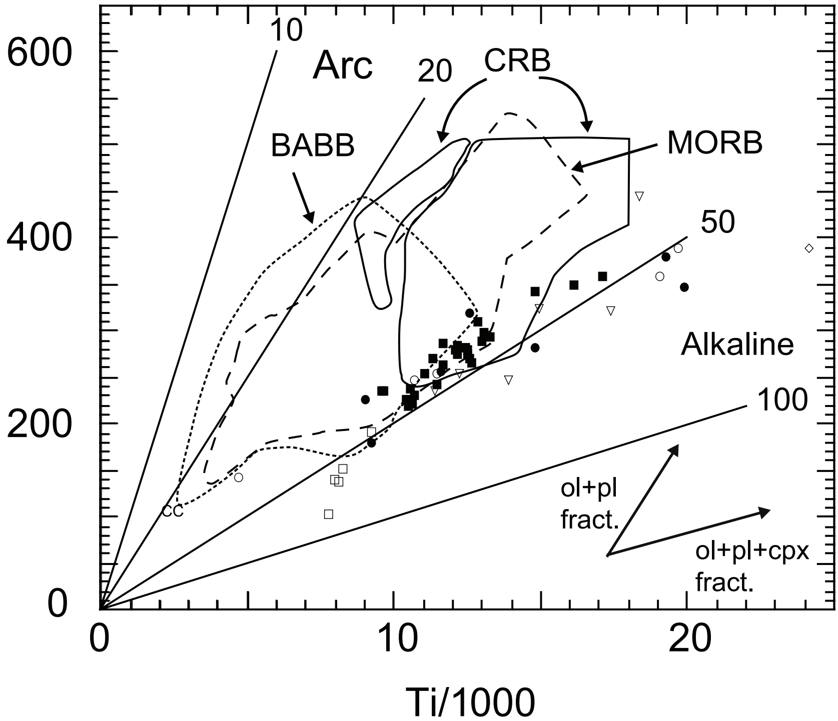

Fig. 13. Ti-V diagram of Shervais (1982). ARC = volcanic arc basalt, MORB = mid-ocean ridge basalt, ALK WPB = alkaline within-plate basalt, BABB = back-arc basin basalt field, CRB = Columbia River flood basalt field. CC = average upper continental crust composition (from McLennan, 2001). See figure 6 for symbol explanation.

tics (Th- and Ce-enrichment and Ta-Nb negative anomaly) result from earlier subduction processes affecting the mantle as concluded by Hon and others (1992), Dostal and others (1989), and Keppie and Dostal (1994) and possibly accompanied by continental crustal contamination. If the original mantle source was depleted, then crustal contamination may be the source of Th enrichment. If the mantle source is more enriched, then the Th is more likely to be derived from the mantle source, without crustal contamination. The discrimination diagrams are interpreted below in the context of these two hypotheses.

The discrimination diagrams, as with the normalized diagrams, invite multiple interpretations; samples plot across multiple fields or in overlap fields. On two of the Th-based diagrams (figs. 10 and 12,) SLV-II, WB, FPV, and FL samples plot along trends of variable Th-enrichment typical of a volcanic arc or back-arc basin setting, and are consistent with the pattern seen in the MORB-normalized diagrams. SLV-I samples are less enriched in Th and plot at the low-Th end of these trends and in many cases are within the N-MORB field from which these trends originate. On the Ce/Nb-Th/Nb diagram (fig. 15) all samples are scattered along a trend of increasing Th, but mainly fall in the back-arc basin field, rather than the arc field. Further, they do not show the same concomitant increase in Ce with Th typical of arc basalts. In the first two diagrams (figs. 10 and 12) the continental crustal contamination vector (indicated by the composition of continental crust, CC) is sub-parallel to the arc vector while the two vectors diverge in the Ce/Nb-Th/Nb diagram. This allows the possibility that the arc

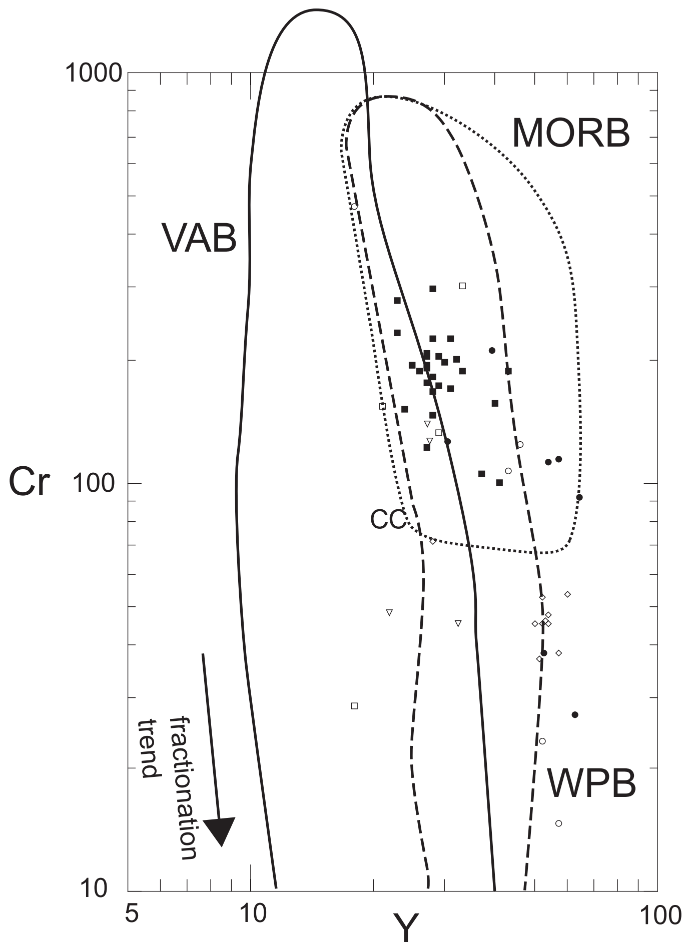

Fig. 14. Cr-Y diagram of Pearce (1982), VAB = volcanic arc basalt, MORB = mid-ocean ridge basalt, WPB = within-plate basalt. CC = average upper continental crust composition (from McLennan, 2001). See figure 6 for symbol explanation.

character displayed in these diagrams may be the result of AFC, and is supported by the AFC-parallel distribution (but not arc trend) of the samples seen in the Ce/Nb-Th/Nb diagram.

On all non-Th based discrimination plots (figs. 9, 11, 13, and 14), SLV-I and FL samples plot relatively uniformly in within-plate continental tholeiite fields, although some plot in the overlap fields with E-MORB, N-MORB, and volcanic arc basalts. SLV-II, WB, and FPV samples are more scattered and generally define linear trends that originate in the within-plate continental tholeiite field and trend toward the composition of upper continental crust (CC). On the Ti-Zr-Y diagram (fig. 9), most samples plot in the WPB field (which includes within-plate alkaline basalts) while some plot in the arc field and arc/MORB overlap field. Two samples plot outside of the defined fields altogether, near the composition of continental crust. It should be noted that continental tholeiites also plot in the CAB and arc/MORB overlap fields (Holm, 1982). All samples with measurable Nb have Y/Nb ratios of 2.5 or greater, consistent with within-plate continental tholeiites, rather than within-plate alkaline basalts. The

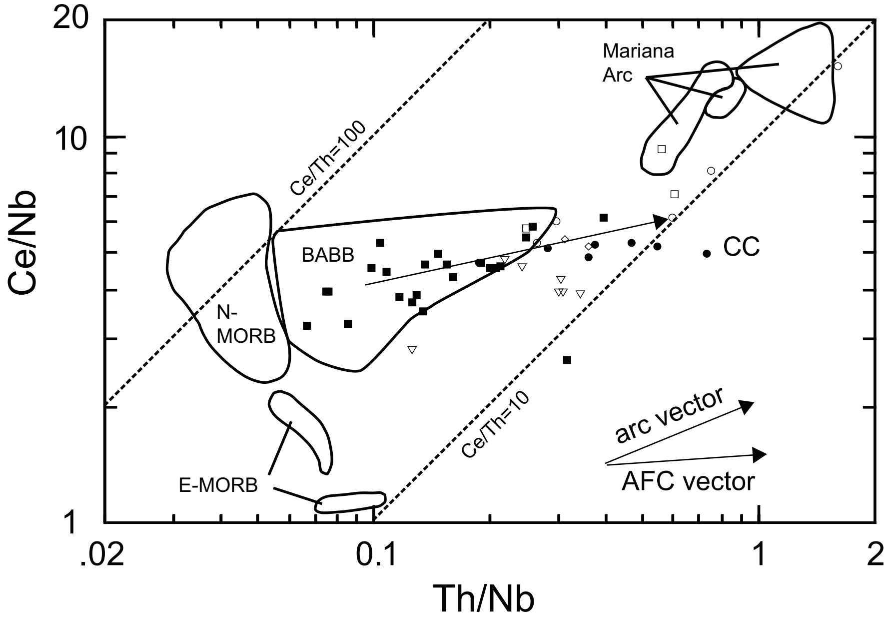

Fig. 15. Ce/Nb vs. Th/Nb diagram of Saunders and others (1988). N-MORB = depleted mid-ocean ridge basalt field, E-MORB = enriched mid-ocean ridge basalt field, BABB = back-arc basin basalt field. CC = average upper continental crust composition (from McLennan, 2001). See figure 6 for symbol explanation.

Nb-Zr-Y diagram (fig. 11) also yields similar results, although most samples plot in the overlap field of WPT and VAB, while only a few plot exclusively in the WPT field.

The Ti-V and Cr-Y diagrams (figs. 13 and 14) in part contrast with the Ti-Z-Y and Nb-Zr-Y diagrams. Samples mainly plot in overlap fields between MORB, continental tholeiite, and to a small extent, back arc basin basalt, rather than volcanic arc basalt fields. In the Ti-V plot, the uniformity of SLV-I suggests magmas that have experienced approximately equal degrees of partial melting, while other samples (the WB suite, in particular) may have experienced variable, higher degrees of partial melting, driving Ti and V abundances upward and to the right along the olivine, plagioclase, +/− clinopyroxene fractionation trends delineated by Shervais (1982). Back-arc basin

TABLE 5

Nd isotope results from West Branch Volcanics (using 417 Ma model age)

Sample:	$^{143}Nd/^{144}Nd$ sample[1]	Sm ppm, sample	Nd ppm, sample	$^{147}Sm/^{144}Nd$ sample[2]	$^{143}Nd/^{144}Nd$ CHUR, 417 Ma	$^{143}Nd/^{144}Nd$ initial	εNd initial
FPV-01-21	0.512804 ± 8	5.63	18.32	0.307314	0.512113	0.512308	+3.8
DA	0.512756 ± 8	8.06	28.75	0.280348	0.512113	0.512303	+3.7
CSK/P-001b	0.512724 ± 7	9.38	34.83	0.269308	0.512113	0.512289	+3.5
CSK/P-003	0.512707 ± 11	4.31	14.63	0.294600	0.512113	0.512231	+2.3
FW-02-21	0.512730 ± 7	8.30	28.56	0.290616	0.512113	0.512261	+2.9

[1] Laboratory uncertainty is 2σ and error value is to the 6th digit right of decimal place.
[2] The $^{147}Sm/^{144}Nd$ ratio was calculated using factor of 0.605 ($^{147}Sm/^{144}Nd = Sm_{ppm,sample}/Nd_{ppm,sample}*.605$).

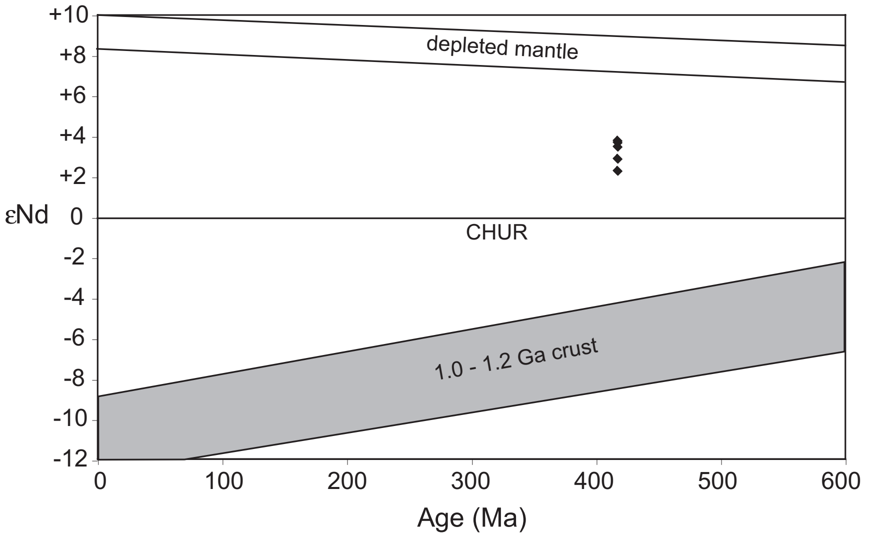

Fig. 16. Plot of εNd vs. age for West Branch samples (417 Ma model age). Depleted mantle curve from DePaolo (1981). 1.0–2.0 Ga crust curve from Samson and others (2000).

basalts may also have relatively high Ti-V ratios, similar to MORB and continental tholeiites. However, suites of such rocks tend to plot in both arc and MOR fields and have relatively low absolute abundances of both Ti and V (Shervais, 1982); no samples shown here have arc-like Ti-V ratios and some have relatively high Ti and V concentrations. On the Cr-Y diagram most samples plot in the WPB field, although most also plot in the MORB overlap, and some in the VAB field. Almost all samples in figure 14 appear to be derived from the lower degree of partial melting associated with either MORB or within-plate settings, and unrelated to supra-subduction zone processes.

A MOR setting is also indicated by some samples, on some diagrams (figs. 9, 10, 12, 13, and 14), although there is much overlap in fields; MORB is not uniquely indicated. On geological grounds, a MOR setting is considered unlikely given that the related coarse-grained clastic and carbonate marine sedimentary rocks are generally associated with a continental margin or shallow cratonal sea, and the lack of most MOR elements such as sheeted dikes, layered gabbro, ultramafic rock, or chert.

Overall, the geochemical patterns provide strongest evidence for either a supra-subduction or within-plate tectonic setting, although complications exist for both. A volcanic arc is complicated by the lack of arc signal in the non-Th based discrimination diagrams, while a within-plate setting would require a process to enrich Th in these rocks. Previous interpretations (Hon and others, 1992; Keppie and Dostal, 1994; Schoonmaker and others, 2005) that continental crustal contamination may have anomalously enriched Th may be supported by moderately positive ε_{Nd} values of the West Branch Volcanics, if derived from originally depleted mantle. Additionally, the area was subject to pre-Siluro-Devonian subduction processes that may also provide such a mechanism. The Ordovician Dry Way Volcanics in the Ripogenus Gorge show anomalous Th-enrichment and have been interpreted to form in an accretionary prism (Schoonmaker and Kidd, 2006) and the nearby Hurricane Mountain mélange in the Lobster Mountain Anticlinorium likely represents the suture between pre-Siluro-Devonian Laurentia and Ganderian crust (Red Indian Line). The moderately positive ε_{Nd} values are also similar to or slightly less positive than older (~467 Ma) mafic rocks from the nearby Bald Mountain massive sulfide deposit and Winterville Formation in the Pennington Mountain Anticlinorium and Mount Chase Deposit in the Munsungun Anticlinorium, which have ε_{Nd} values that range from about +3 to +6 (Ayuso and Schulz, 2003). The West Branch Volcanics must have tapped the same mantle that generated these older volcanics and the slightly lower moderately positive ε_{Nd} values of the West Branch rocks may be the result of some component of crustal mixing.

A third possibility that is largely consistent with the geochemical data is that these rocks were erupted during early stages of rifting in a backarc setting during slab-roll back, but never fully developed into a true backarc basin. Such a setting is suggested by the Ti-V and Ce/Nb-Th/Nb diagrams (figs. 13 and 15) where samples plot in back-arc fields. Similarities in geochemistry are seen in the Honeysuckle beds (volcanics) of eastern Australia, which are interpreted to have formed in an incipient back-arc basin (Dadd, 1998) and show mixing of enriched mantle-derived mafic rocks and VAB. Further, the early stages of Lau Basin magmatism are also broadly similar. However, the early Lau basin magmatic rocks differ significantly from the Maine rocks in that they vary from MORB to VAB (instead of WPB to VAB) and were built on oceanic crust, rather than continental (Ganderian) crust. The variation in the Lau Basin is interpreted to be the result of mixing of depleted sub-ocean mantle and arc-derived fluids (Hergt and Farley, 1994; Hawkins, 1994). In the case of Maine, application of this scenario involves mixing of enriched sub-continental mantle and arc fluids, which could have resulted in the mixed signal observed.

TECTONIC MODELS

Introduction

From the preceding discussion of stratigraphy and igneous geochemistry, the following general conclusions may be drawn. During the late Silurian and early Devonian, the stratigraphic sequences of the northern Maine inliers indicate a period of shallow water deposition that was followed by more rapid subsidence and concurrent mafic volcanism that occurred *prior* to the onset of Acadian deformation and widespread bi-modal magmatism. Following a period of subaerial exposure (Taconic/Salinic unconformity at the top of the Dry Way Volcanics), near shore conglomerates and reefal limestones were deposited during the latest Silurian to earliest Devonian (Ripogenus, lower part of The Forks, and the Chandler Pond formations, and unnamed coarse clastics in the Shin Pond/Stacyville area), followed by brief uplift and erosion (disconformity at orthoquartzite in the Ripogenus Formation and conglomerates in the Chandler Pond Formation and near White Horse Lake). Next, rapid regional subsidence with fine-grained and turbiditic sedimentation and volcanism occurred (siltstone section of the Ripogenus Formation, West Branch Volcanics, and Frost Pond Shale; the upper part of the East Branch Group and Spider Lake Volcanics; upper part of The Forks Formation and Fish Pond Volcanics), in a within-plate, volcanic arc or backarc setting, followed by orogenic flysch/molasse deposition of the Seboomook Group and Matagamon Sandstone. Syn-Acadian magmatism is evidenced by mutually crosscutting relationships between subsequent Traveler-Katahdin and Flagstaff Lake rocks and Acadian deformation. Any reasonable tectonic model proposed for this interval in northern Maine should be consistent with these geological constraints.

A controversial issue is the nature of Acadian convergence and subduction polarity, and several competing hypotheses have been presented in the literature for various regions (for example, Bradley, 1993; Keppie and Dostal, 1994; van Staal and others, 1998; Murphy and others, 1999; Eusden and others, 2000; Tucker and others, 2001; Bradley and Tucker, 2002; Schoonmaker and others, 2005; West and others, 2007; van Staal and others, 2009). It has been clearly shown that the Acadian deformation front migrated northwesterly across Maine during the late Silurian through early Devonian time (Bradley and others, 2000). This places the orogenic front to the southeast of the northern Maine inliers, prior to its arrival in the Early Emsian. On *a priori* grounds, and assuming the Acadian suture lies southeast of the Maine inliers and that Ganderian crust underlies much of Maine, this requires that the Siluro-Devonian sequences of the northern Maine inliers must either have been emplaced in the backarc region of a northwest-dipping subduction zone, or the trench and outer trench slope region of a southeast-dipping subduction zone. Equivocally, both east- and west-verging structures have been documented in various parts of the orogen (Tucker and others, 2001; references in Eusden and others, 1996).

We evaluate four possible Acadian tectonic scenarios (fig. 17) that might explain the late Silurian–early Devonian geology of northern Maine. Our evaluation is weighted in favor of the geology exposed in the Maine inliers, although evidence from other parts of the Acadian orogen is cited in support or contradiction of each model. Model 1 proposes that early Devonian, bimodal magmatism in northern Maine (Piscataquis Volcanic Belt) may be the result of incipient slab failure (continental lithosphere extension and detachment) in the outer trench slope of a southeast-directed (modern coordinates), subducting Laurentian (+Gander) continental margin during the Acadian Orogeny similar to the models proposed by Robinson (1993), Robinson and others (1998), Bradley and others (2000), Tucker and others (2001), Model A-B of Bradley and Tucker (2002), and Schoonmaker and others (2005). Model 2 explains the northwest migrating Acadian front to be the result of back-arc deformation similar to the Andean Sierras Pampeanas, or cratonal Laramide Orogeny as suggested by Murphy and others (1999), Eusden and others (2000), Model C-D of Bradley and Tucker (2002), and van Staal and others (2009). Related magmatism may have resulted from the hydration of lithospheric mantle above the contact with the subducting slab (for example, Humphreys and others, 2003). Model 3 envisages the northwest migrating Acadian front occurring in the back-arc region above a northwest-dipping plate, while associated magmatism and subsidence is related to incipient opening of a short-lived back-arc basin in northern Maine, or extension during slab roll-back, similar to that proposed by West and others (2007). Model 4 is based on the "Moluccan-style" dual subduction model proposed by Bradley (1993), Eusden and others (2000), and Bradley and Tucker (2002).

Model 1—Slab Detachment (Southeast-Dipping Subduction Zone)

Model 1 (fig. 17A) requires tectonic subsidence and extension of the amalgamated Laurentian+Ganderian margin as it entered the outer trench slope region of an Acadian subduction zone dipping southeast (modern coordinates) beneath the Avalonian terrane during the early stages of Acadian Orogeny in northern Maine, whose suture lies southeast of the Maine inliers. Lower plate failure of a southeast-dipping plate would involve the following events: 1) shallow-water deposition of the Ripogenus Formation and equivalent rocks on the Gander-modified eastern Laurentian margin, part of the lower plate as it approached the Acadian subduction zone; 2) brief sub-aerial exposure during the passage of a peripheral flexural bulge; 3) subsequent, abrupt change to deeper-water sedimentation as the margin underwent rapid subsidence synchronous with normal faulting and pre-orogenic mafic magmatism of the West Branch Volcanics as the lower plate underwent extension in the outer trench slope region; 4) closely followed by flysch deposition (Seboomook Formation) and widespread bimodal magmatism (for example, Moxie Gabbro, granitic Katahdin Batholith, Traveler Rhyolite, Flagstaff Lake Igneous Complex) contemporaneous with the onset of Acadian deformation (in the trench and vicinity, including the initial accretionary thrust and fold belt of the inner trench slope). Similar relationships are seen in The Forks area of the Lobster Mountain Anticlinorium, the Munsungun Anticlinorium and the northwest limb of the Weeksboro-Lunksoos Anticlinorium,

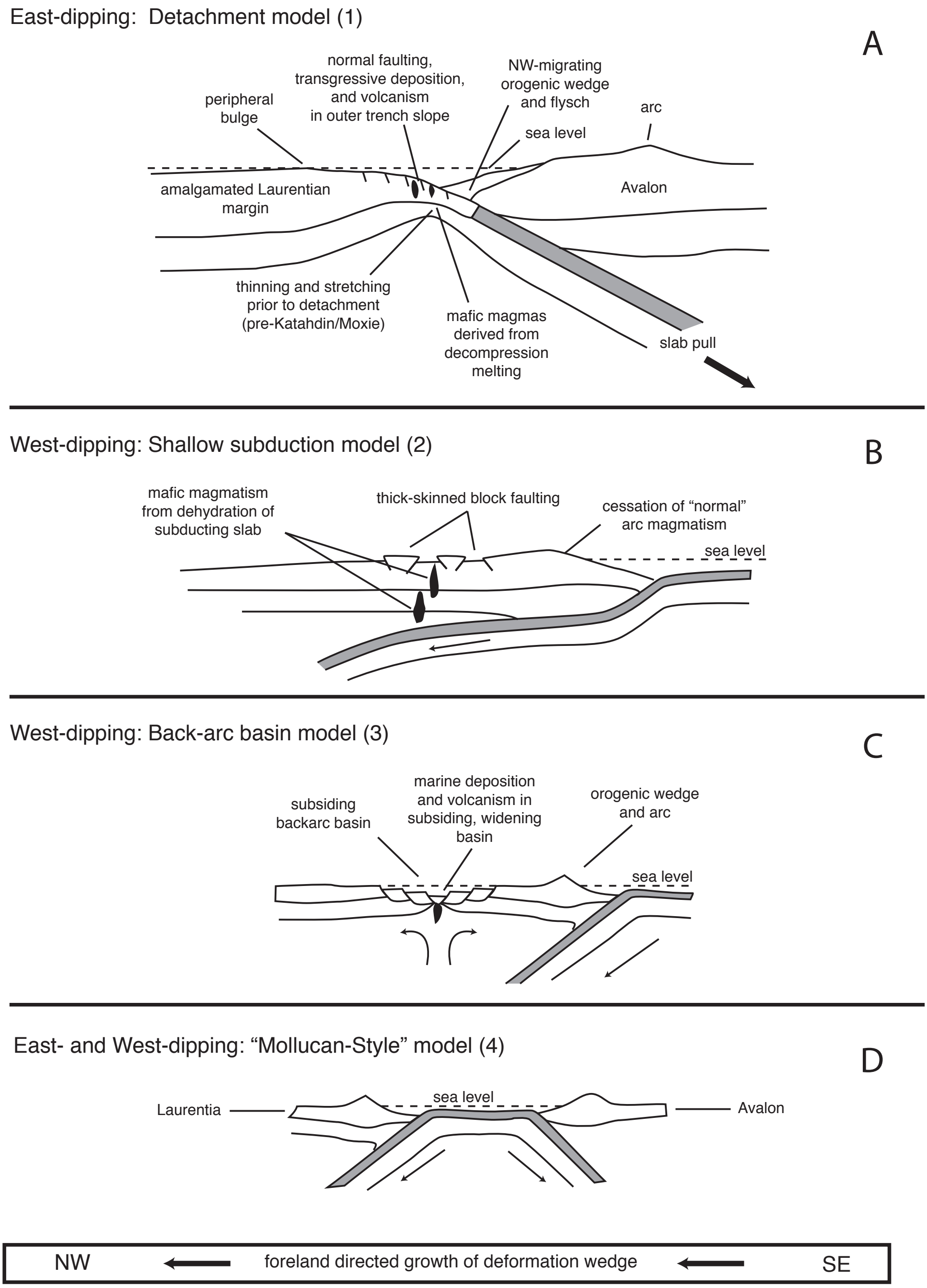

Fig. 17. Tectonic scenarios prior to the onset of Acadian Orogeny in northern Maine (Pre-Emsian). (A) southwest-directed subduction. (B) northwest-directed, "Laramide-style" shallow subduction. (C) northwest-directed subduction with embryonic back-arc basin. (D) "Mollucan-style" dual subduction.

indicating a regional consistency to this event. Model 1 is an instantaneous depiction of the situation during pre-Emsian early Devonian, prior to Katahdin/Moxie/Flagstaff Lake magmatism that subsequently (Emsian) intruded the overriding orogenic wedge and northwest-migrating flysch deposits. This subsequent magmatism is illustrated in figure 7 of Bradley and Tucker (2002) and figure 1 of Schoonmaker and others (2005).

Importantly, this interpretation requires that the "arc" geochemical signal in some of the samples is not the result of subduction processes above a westward dipping slab beneath the amalgamated Laurentian margin. There are several potential difficulties with this model that have been discussed by previous workers (for example, van Staal, 2009). One interpretation, based on reprocessing of the Lithoprobe seismic line in Newfoundland, suggests reflectors that may be Avalonian crust thrust beneath Ganderia/Laurentia along a west-dipping boundary (van der Velden and others, 2004), and may be supported by a retro-deformation of the Lyme Dome in Connecticut (Wintsch and others, 2008) and west-over-east sense-of-shear in the Burlington mylonite between the Nashoba Terrane and Avalon terrane (Kohut and Hepburn, 2003). Also, the modern relative position (from east to west) of the Pocologan metamorphic suite, and Kingston and Mascarene terranes have been interpreted as fore-arc high pressure metamorphic, arc and back-arc terranes, respectively (Fyffe and others, 1999; Barr and others, 2002; White and others, 2006). An eastward-dipping subduction zone is difficult to reconcile if their current configuration represents their original relative positions. However, these terranes are complexly fault-bounded and may be shuffled so that the original relationships are difficult to infer (White and others, 2006). Another issue is the length of time of Acadian magmatism that may have begun as early as 419 Ma (Ludlovian conodonts beneath the West Branch flows in the Ripogenus Formation) and continued into the middle Devonian (Bradley and others, 2000). Other slab break-off events have been over shorter time scales (for example, Whalen and others, 2006; Yuan and others, 2010). This suggests that if slab break-off occurred, it may have been complex, possibly requiring an incomplete and/or episodic failure, or multiple failures of the slab, although this is difficult to evaluate with this data set. Finally, van Staal and others (2009) and Reusch and van Staal (2011) suggest that the magmatic rocks emplaced prior to the arrival of the Acadian deformation front (for example, West Branch and correlatives) may not be Acadian, but instead related to late stage Salinic slab break-off. Such a scenario might explain the within-plate geochemical signal, but this extends the effects of the Salinic outside of established ages of this event. Further, this would not apply to the Flagstaff Lake rocks that are even younger and show less arc character than the older WB and SLV rocks (figs. 8C, 9, 11, and 13).

Model 2—Shallow Subduction (Northwest-Dipping Subduction Zone)

Model 2 (fig. 17B) involves flat-slab subduction, based on Andean- or Laramide-style tectonics. According to this model, west-directed subduction occurred as the Avalon terrane approached the eastern margin of the Gander/Laurentian margin resulting in construction of the Kingston arc, Mascarene back-arc relationships cited above (van Staal, 2007; van Staal and others, 2009; Hibbard and others, 2010). Further, deposition of the Arisaig Group has been interpreted to represent a period of subsidence of the Avalon terrane (Waldron and others, 1996), which van Staal and others (2009) and Hibbard and others (2010) suggested represents subsidence as an Avalon (upper-plate) underwent loading during its approach to the Acadian orogen. Shallow subduction, initially proposed by van Staal and others (1998) and Murphy and others (1999), allows for subsequent northwest migration of a back-arc (located in the foreland of the upper plate) deformation front with associated magmatism, based on the examples of the flat-subduction sections of the Andean Orogeny and the Laramide Orogeny (van Staal and others, 2009). Limited volcanism locally accompanied foreland deformation in these regions (for example, Lipman, 1992; Kay and Gordillo, 1994), and may account for the potential arc aspect of the Piscataquis belt rocks.

In the context of model 2, the Acadian Orogeny in northern Maine shows some similarities with the Andean and Laramide orogenies. According to model 2, the upper plate is represented by the amalgamated Laurentian margin, whose leading edge was Ganderia (and the coastal Maine magmatic belt). Avalon, to the southeast, approached as a result of northwest-directed subduction beneath this margin. The resulting orogenic belt originated southeast of the northern Maine inliers and advanced northwestward, towards the back-arc during slab flattening. Subsequent magmatism of the West Branch and related volcanics, and Katahdin and related plutons would have intruded in advance of, and into (respectively), the leading edge of the northwest-migrating orogenic wedge, well in the back-arc position of the upper plate. Broadly, this model resembles those developed for the Laramide foreland and Andean retroarc (for example, Pocho) flat slab-influenced orogenies.

In the eastern Rocky Mountains, mechanisms for magmatism above a shallowly subducting slab are controversial (for example, Humphreys and others, 2003; McMillan and others, 2003; Lee, 2005; McMillan and Lawton, 2006; Wells and Hoisch, 2008), but most likely involve the input of hydrous fluids from the subducting slab into the backarc (foreland) region, which has produced arc-like magmatism far from the normal arc axis. During this stage, melting was limited due to the lack of asthenospheric mantle above the slab and occurred at greater depths. Volcanics are generally calc-alkaline and contain evidence for hydrous fluid interactions (Miller and others, 1992; Lipman, 1992; Humphreys and others, 2003; Lee, 2005; Wells and Hoisch, 2008). Subsequent foundering and steepening of the slab allowed an influx of hot asthenospheric mantle material beneath the hydrated lithosphere that produced post-deformation, strongly alkaline magmas (Lipman, 1992).

Similarly, in the current flat slab-influenced Sierras Pampeanas of Argentina (29°-33°S. lat.), volcanics having an arc signature (for example, Pocho Volcanic field), including hornblende-bearing, low TiO_2 (dominantly <1%) mafic rocks and shoshonites erupted during or near the interval of uplift (from ~10-2 Ma) resulted from an influx of subduction fluids into the back-arc (retroarc) region as the subducting plate flattened (Kay and Gordillo, 1994; Kay and Abruzzi, 1996; Kay and others, 2006). Similarly, in the region of 33° to 39°S (latitude), where flat subduction was present during the late Miocene and Pliocene, foreland (retroarc) volcanism of the Payenia volcanic field occurred during two intervals: late Miocene and Pliocene to Quaternary (for example, Ramos and Kay, 2006). The first episode that occurred during uplift of the Sierra de Chachahuén has arc characteristics, including hornblende-bearing basalt-andesites, significant pyroclastic deposits, and is related to a brief period of slab flattening. Subsequently, post-deformation, alkaline, within-plate lavas were erupted as the slab re-steepened during the Pliocene and early Quaternary (Ramos and Kay, 2006; Kay and others, 2006). In both the Andean and Laramide orogenies, arc-like high K, calc-alkaline volcanism, non-marine basin sedimentation, and foreland deformation are produced during slab flattening, while alkaline within-plate magmatism results from subsequent foundering of the slab following deformation and uplift.

In both the Sierras Pampeanas of the eastern Andes and the Laramide foreland region of the Western Cordillera, flat slab deformation has resulted in thick-skinned uplift and exposure of craton basement blocks separated by deep non-marine basins into which thick sequences of immature fluvial sandstones and conglomerates are deposited (for example, Jordan and Allmendinger, 1986; Miller and others, 1992; Ramos, 2008).

There are several significant differences between the Maine Acadian and Laramide/Andean orogenies: 1) abundant late Silurian and early Devonian magmatism extends for over a thousand kilometers in New England and Canada, while Laramide and Andean backarc magmatism is scattered at various distances across the strike of the orogen, resulting from a gradual migration of arc volcanism towards the foreland (retroarc) as the slab shoaled. The degree of cross-strike plutonism of Acadian plutons is relatively small with the Piscataquis Volcanic Belt and Greenville Plutonic Belt at present approximately 100 to 200 km from the strike of the Coastal Volcanic Belt. In the Rocky Mountain foreland especially, volcanic and plutonic rocks are spatially restricted and not linearly distributed (Miller and others, 1992). Further, deformation and magmatism of the Laramide and Sierra Pampeanas regions is occurring/occurred >1000 and 500 to 800 km in the back-arc regions, respectively, although the geometry of the slab might differ (for instance, the Laramide slab may have foundered to a greater distance than the Acadian slab). 2) Tertiary magmatism in the Rocky Mountain foreland and late Miocene to Pliocene retroarc magmatism in the Andes is composed of initially high K, calc-alkaline rocks related to slab flattening, followed by highly alkalic magmas associated with slab foundering (Lipman, 1992; Kay and others, 2006). In northern Maine, the earliest volcanics have a significant within-plate character, and show limited arc influence, and occurred shortly before the arrival of the deformation front. If they were emplaced above a northwest-dipping slab, they ought to be associated with initial slab shallowing magmatism (that is, show the effects of subduction fluids), not subsequent foundering of the slab. 3) Slab flattening created uplift and exposure of basement blocks as magmatism migrated into the foreland regions during the Laramide and Andean orogenies, while the northern Maine stratigraphy records regional subsidence at the time of initial magmatism. 4) Sedimentation in the Andes and Laramide foreland is composed of non-marine sandstones and conglomerates that interfinger with the foreland volcanics in deep, discrete basins, separated by uplifted blocks of basement. In northern Maine, mature marine sediments were deposited in a regionally extensive subsiding basin at the time of volcanism (for example, West Branch), followed by a regionally extensive Seboomook basin. 5) Syn-deformational magmatism associated with the Andean and Laramide orogenies is strongly marked by the presence of hydrous fluids (for example, hornblende-bearing calc-alkaline volcanics, Kay and Gordillo, 1994; Humphreys and others, 2003; Lee, 2005) and extensive pyroclastic deposits, while the Spider Lake Volcanics and West Branch volcanics were dry and hot. A distinct lack of ash deposits, explosive volcanism, and hydrous phenocryst phases characterize the northern Maine rocks (Fitzgerald, ms, 1991). The Flagstaff Lake gabbros do contain hornblende, but they show significant textural evidence of contamination with country rock (Nielsen and others, 1989).

Van Staal and others (2009) argue that pockets of sub-Laurentian mantle were trapped above the subducting Avalon slab, which provided a mantle source for the mafic rocks of the Piscataquis belt. However, it is difficult to reconcile the abundant early Devonian magmatism in Maine and New Brunswick with such a limited mantle source.

Model 3—Back-Arc Basin (Northwest-Dipping Subduction Zone)

The third model, a short-lived embryonic back-arc basin is illustrated in figure 17C. This model has not been previously proposed, although it is similar to a model proposed by West and others (2007) to explain the origin of the Lincoln syenite, and relies on slab roll-back of a west-dipping subduction zone. In this model, a subducting slab extending westward beneath the Laurentian-Gander crust undergoes foundering and slab rollback, creating backarc extension, subsidence, and within-plate magmatism in the northern Maine inliers. The rapid succession of thrust shortening and northwest migration of the Acadian deformation front requires that extension was short-lived and the setting changed to convergent shortening for the rest of the Acadian event. The pre-Emsian northern Maine stratigraphy and facies succession, and within-plate and possible VAB character of the volcanics is consistent with sedimentation associated with lithospheric extension, and associated subsidence and magmatism. In this model, subsidence immediately prior to and accompanying volcanism can be readily accounted for by rifting, and the preceding brief exposure and disconformity in the shelf sediments of the Ripogenus and equivalent units could be attributed to the thermal effect of upwelling mantle, before mechanical stretching of the lithosphere and subsidence became dominant.

The geochemistry of the northern Maine volcanics is in part consistent with a backarc interpretation. On several discrimination diagrams the backarc basin field overlaps with the continental tholeiite field (for example, Ti-Zr-Y, Ti-V, Hf-Th-Nb). In most backarc basin settings built on oceanic crust, basalt geochemistries show a range of compositions between volcanic arc basalts and MORB (for example, Saunders and Tarney, 1984; Hawkins, 1994). In this case, the upper plate would be the amalgamated Laurentian continental margin. In northern Maine, MORB compositions are indicated on some plots but within-plate tholeiites are more common, possibly explaining this difference in mantle source. However, the regional setting and associated facies of the lower Devonian volcanics could only be associated with early rifting stage of backarc opening. Compositions of known backarc magmas are strongly arc-like in composition (Weaver and others, 1979; Hawkins, 1995), which contrasts with the geochemistry of the Piscataquis Volcanic Belt.

Also problematic is that the infilling of the basin by flysch turbidites of the Seboomook and equivalents requires a sedimentary source other than any associated arc. In backarc basins, at least the initial overlying flysch contains volcanogenic detrital material and ash derived from the nearby arc; the Seboomook Formation, Frost Pond, and Ripogenus formations (as well as other correlative rocks in the other inliers) lack such material. This model is also inconsistent with nearly 40 million years of magmatism in the Piscataquis Volcanic and Greenville Plutonic belts; with even a short period of slab rollback it is difficult to reconcile with the well-constrained, long-term northwestern advance of the Acadian front. Possibly this may be explained by episodic foundering of the slab over relatively short intervals of time, related to heterogeneities in the subducting oceanic lithosphere.

Model 4—"Moluccan-Style" Dual Subduction

A Moluccan-style model has been proposed (for example, Model E-F of Bradley and Tucker, 2002; Bradley, 1993; Eusden and others, 2000), where northwest-directed subduction beneath the Laurentian margin occurred while concurrent southeast-directed subduction occurred beneath the Avalon plate (fig. 17D). This model is based on the assumption that the Piscataquis Volcanics are arc-related (for example, Kusky and others, 1994), which is potentially the case given the equivocal nature of the magmatic rocks of the northern Maine inliers and New Brunswick. Additionally, the Lebanon Gabbro may have also resulted from arc processes (Bowman and others, 2007). Eusden and others (2000) suggested that the lack of widespread arc volcanics may have resulted from "buoyant" subduction after Cross and Pilger (1982). Such a model does satisfy much of the evidence in the Acadian orogen (for example, possible arc-affinity of Piscataquis rocks on the NW side, NW-migrating deformation front on the SE side, both east- and west-verging structures) but also suffers from most of the possible problems of both the east- and west-dipping models (for example, forearc-arc-backarc geometry associated with an east-dipping slab, and the abundant within-plate magmatism and regional subsidence in the Piscataquis Volcanic Belt above a shallow west-dipping slab). As such, this requires a complicated confluence of many processes, in stronger violation of the law of parsimony than any of the other three models examined here.

CONCLUSIONS

The Acadian orogeny is complex and even first-order questions concerning its evolution are controversial, and several competing tectonic models have been proposed to explain various aspects of it. Complicating matters, much of the geochemical data presented here is transdiscriminant, indicating multiple possible processes and none of the models presented here explains uniquely and fully the geochemical and stratigraphic data presented. Further, other aspects of the orogen outside of the Maine inliers also give conflicting indications.

The Siluro-Devonian stratigraphic sections of the northern Maine inliers indicate a period of shallow marine deposition followed by a rapid increase in subsidence accompanied by mafic magmatism, which has both within-plate and arc geochemical characteristics, being derived either from a depleted, or from a moderately enriched mantle. The within-plate character is more prevalent in the geochemical patterns and difficult to explain in an arc environment, but may be related to incipient backarc extension. The arc character is almost exclusively defined by Th, Nb, and Ta concentrations and may be explained, in a within-plate environment, by derivation from a previously subduction-modified mantle, and possibly also affected by crustal contamination.

Model 1 most closely satisfies the geochemical and stratigraphic data for the Maine inliers, although it may conflict with some evidence outside of the area (for example, the Kingston-Mascarene relationships). It also requires a process of Th-enrichment in the subcontinental mantle other than assimilation and fractional cystallization, possibly pre-Silurian subduction associated with closure of the Iapetus Ocean separating Laurentia and Gander along the Red Indian Line.

Model 2 explains the arc character seen in the volcanic rocks of the Maine inliers, but is inconsistent with the strong within-plate character of the volcanic rocks. This may be explained if much of the Piscataquis Volcanic belt is related to late stage Salinic slab breakoff but however, does not explain the chemistry of the Flagstaff Lake Igneous Complex. This model is also inconsistent with subsidence and marine deposition of the Ripogenus Formation and equivalents; backarc regions above shallowly subducting slabs typically create uplift, basin and range topography, and terrestrial coarse-grained deposition.

Model 3 provides a mechanism to produce the transdiscriminant geochemistries between VAB and WPT seen in the geochemical diagrams presented, and is consistent with extension and the stratigraphic succession seen in northern Maine. However, the lack of a true oceanic basin or significant MORB signature requires that only a short period of extension occurred, inconsistent with the extended period of magmatism in the region.

Model 4, encapsulating aspects of east- and west-directed subduction, explains much of the data from northern Maine and the region, but also suffers from almost all of the problems associated with those models, requiring a perhaps unlikely set of circumstances to occur.

ACKNOWLEDGMENTS

The authors thank Cees van Staal, Dykstra Eusden, and an anonymous reviewer for critical comments that have significantly improved this paper. We also thank Dwight Bradley for helpful comments on the nature of Acadian orogenesis. AS and WSK would also like to thank Dee Caldwell (posthumously) for his wonderful company and lessons in the pronunciation of Maine place names at the Boom House during collection of the West Branch samples. The analyses for Nd isotopes were made possible by funds from contributions to the Geology account at the University at Albany Foundation; these contributions are gratefully acknowledged.

Appendix 1

analytical methods

The West Branch analyses reported in Schoonmaker and others (2005) include trace element and rare earth elements obtained using X-ray fluorescence (XRF) and inductively coupled plasma-mass spectrometry (ICP-MS). Reported major elements and Zr values in table 1 are XRF results. All other reported elements are from ICP-MS. Samples were chosen to minimize alteration and veins. Chips were hand picked at the University at Albany to avoid weathered surfaces, veins and interior inclusions; powders were ground and analyzed (XRF and ICP-MS) at Washington State University's GeoAnalytical Laboratory (WSU). Samples were sent to WSU in two batches, five months apart; both batches included the Palisades Sill standard PAL-889. We compared the XRF analyses of PAL-899 at WSU with an XRF analysis from the University of Massachusetts (UMass) with the following percent variations (% variation=100*[WSU—UMass]/UMass; batch 2 in parentheses): TiO_2: 0.5% (0.5%), Cr: 0.6% (0.8%), V: 2.6% (3.0%), Zr: 6.5% (6.5%). Similarly, the two ICP-MS analyses of PAL-889 were compared to an INAA analysis from Cornell University, with the following percent variations: La: 0.5% (5.0%), Ce: 8.3% (9.8%), Nd: 6.8% (7.3%), Sm: 2.5% (1.5%), Eu: 10.5% (5.6%), Tb: 3.5% (0.2%), Yb: 6.3% (5.7%), Lu: 3.2% (1.4%), Ba: 4.8% (5.7%), Th: 0.4% (3.2%), Hf: 0.1% (1.2%), Ta: 3.7% (6.0%), U: 8.9% (10.2%), Cs: 10.4% (11.8%), Sr: 3.7% (7.9%).

The Fish Pond Volcanics, reported in Gregg and Reusch (2007), were analyzed during the winter of 2007 by X-ray fluorescence (XRF) spectrometry on the University of Maine at Farmington's Bruker System S4 Pioneer instrument. Samples were crushed into approximately 1 cm^3-sized chips. Samples displaying the least amount of weathering were then milled into fine powders using a tungsten carbide mill. The powders were fused into glass pellets on a Phoenix Tm 3000 Fusion machine. Subsequently, chips from samples SUVM-7, SUVM-10, SUVM-12a, and SUVM-18 were sent to ACME Analytical Laboratories LTD., 852 E. Hastings St., Vancouver, BC for analysis of trace and rare earth elements by inductively coupled plasma mass spectroscopy. The samples were received on 2007 April 4. Prior to trace element analysis by ICP-MS, 0.50 g powdered sample was leached with 3 mL of a $HCl\text{-}HNO_3\text{-}H_2O$ solution (2-2-2) at 95 degrees C for one hour, and then diluted to 10 mL. In the analyses for rare earth elements, also done by ICP-MS, 0.200 g powdered sample was first subjected to $LiBO_2/Li_2B_4O_7$ fusion.

Bulk-rock major and trace element analyses of the Flagstaff Lake samples were conducted by Mike Dorais and Chris Spencer using XRF and ICP-MS methods. XRF analyses were made with a Siemens SRS 303 at Brigham Young University using fused disks for major elements and pressed powder pellets for trace elements. Additional trace elements were determined by ICP-MS at ALS Chemex at Reno, Nevada. Reported major elements, Nb, V, Cr, and Ni in table 3 are by XRF, all other values are by ICP-MS.

Five powder fractions of West Branch Volcanics (FPV-01-02, DA, CSK-001b, CSK-003, and FW-02-21) remaining after trace element analysis were sent to the Syracuse University Radiogenic Isotope Laboratory (SURIL, Dr. Scott Samson) to determine Nd isotopic ratios. Detailed laboratory procedures are described in Samson and others (1995) and used a VG-Sector 54 mass spectrometer. A factor of 0.605 was multiplied by the absolute Sm/Nd abundances from ICP-MS analyses to give $^{147}Sm/^{144}Nd$ ratios. A normalization factor of 0.7219 was used for $^{143}Nd/^{144}Nd$ ratios. A model of age of 417 Ma (early Lockhovian) was chosen for the εNd calculation based on the age of Ludlovian to Lockhovian ages reported for conodonts in the Ripogenus Formation, directly beneath the West Branch Flows (Bradley and others, 2000). Another calculation was made using a 408 Ma (post-Lockhovian) model age to test the significance of uncertainties in the age of the West Branch Volcanics. This resulted in a change in εNd of 0.1 in one sample; other εNd values were unchanged by this recalculation.

References

Ayuso, R. A., 1986, Lead-isotopic evidence for distinct sources of granite and for distinct basements in the northern Appalachians, Maine: Geology, v. 14, n. 4, p. 322–325, http://dx.doi.org/10.1130/0091-7613(1986)14⟨322:LEFDSO⟩2.0.CO;2

Ayuso, R. A., and Schulz, K. J., 2003, Nd-Pb-Sr isotope geochemistry and origin of the Bald Mountain and Mount Chase sulfide deposits, Northern Maine, *in* Goodfellow, W. D., McCutcheon, S. R., and Peter, J. M., editors, Massive sulfide deposits of the Bathhurst Mining Camp, New Brunswick, and northern Maine: Economic Geology Monograph 11, p. 611–630.

Barr, S. M., White, C. E., and Miller, B. V., 2002, The Kingston Terrane, southern New Brunswick, Canada: evidence for an Early Silurian volcanic arc: Geological Society of America Bulletin, v. 114, n. 8, p. 964–982, http://dx.doi.org/10.1130/0016-7606(2002)114⟨0964:TKTSNB⟩2.0.CO;2

Begeal, C. J., Kidd, W. S. F., Schoonmaker, A., Bradley, D. A., and Harris, A., 2004, Ripogenus Formation, Northern Maine—age, sequence stratigraphy, and significance of syn-depositional tectonism: Geological Society of America Abstracts with Programs, v. 36, n. 2, p. 89.

Boucot, A. J., 1962, Appalachian Siluro-Devonian, *in* Coe, K., editor, Some aspects of the Variscan fold belt: ten lectures delivered to the Ninth Inter-University Geological Congress: Manchester, England, Manchester University Press, p. 155–163.
——— 1969, Geology of the Moose River and Roach River synclinoria, northwestern Maine: Maine Geological Survey Bulletin 21, 115 p.
Bowman, J. D., Wintsch, R. P., and Elswick, E. R., 2007, Asthenospheric upwelling and slab roll-back of the subducting Avalon Plate; geochemical evidence from the Lebanon Gabbro, east-central Connecticut: Geological Society of America Abstracts with Programs, v. 39, n. 1, p. 76.
Bradley, D. C., 1983, Tectonics of the Acadian Orogeny in New England and adjacent Canada: Journal of Geology, v. 91, n. 4, p. 381–400, http://dx.doi.org/10.1086/628785
Bradley, D., and Tucker, R., 2002, Emsian synorogenic paleogeography of the Maine Appalachians: The Journal of Geology, v. 110, n. 4, p. 483–492, http://dx.doi.org/10.1086/340634
Bradley, D. C., Tucker, R. D., Lux, D. R., Harris, A. G., and McGregor, D. C., 2000, Migration of the Acadian Orogen and foreland basin across the northern Appalachians of Maine and adjacent areas: United States Geological Survey Professional Paper 1624, 49 p.
Burroughs, W., and Marvinney, R. G., 1981, Reconnaissance bedrock geology of The Forks Quadrangle, Maine: Maine Geological Survey Open File Report, n. 81–10, 1 map, scale 1:62,500.
Cross, T. A., and Pilger, R. H., Jr., 1982, Controls of subduction geometry, location of magmatic arcs, and tectonics of arc and back-arc regions: Geological Society of America Bulletin, v. 93, n. 6, p. 545–562, http://dx.doi.org/10.1130/0016-7606(1982)93⟨545:COSGLO⟩2.0.CO;2J
Dadd, K. A., 1998, Incipient backarc magmatism in the Silurian Tumut Trough, New South Wales: an ancient analogue of the early Lau Basin: Australian Journal of Earth Sciences, v. 45, n. 1, p. 109–121, http://dx.doi.org/10.1080/08120099808728372
DePaolo, D. J., 1981, Neodymium isotopes of the Colorado Front Range and crust-mantle evolution of the Proterozoic: Nature, v. 291, p. 193–196, http://dx.doi.org/10.1038/291193a0
Dorais, M. J., and Paige, M. L., 2000, Regional geochemical and isotopic variations of northern New England plutons: Implications for magma sources and for Grenville and Avalon basement-terrane boundaries: Geological Society of America Bulletin, v. 112, n. 6, p. 900–914, http://dx.doi.org/10.1130/0016-7606(2000)112⟨900:RGAIVO⟩2.0.CO;2
Dostal, J., Wilson, R. A., and Keppie, J. D., 1989, Geochemistry of the Siluro-Devonian Tobique volcanic belt in the northern and central New Brunswick (Canada): tectonic implications: Canadian Journal of Earth Sciences, v. 26, n. 6, p. 1282–1296, http://dx.doi.org/10.1139/e89-108
Eusden, J. D., Jr., Garesche, J. M., Johnson, A. H., Maconochie, J.-M., Peter, S. P., O'Brien, J. B., and Widmann, B. L., 1996, Stratigraphy and ductile structure of the Presidential Range, New Hampshire; tectonic implications for the Acadian Orogeny: Geological Society of America Bulletin, v. 108, n. 4, p. 417–436, http://dx.doi.org/10.1130/0016-7606(1996)108⟨0417:SADSOT⟩2.3.CO;2
Eusden, J. D., Jr., Guzofski, C. A., Robinson, A. C., and Tucker, R. D., 2000, Timing of the Acadian Orogeny in northern New Hampshire: The Journal of Geology, v. 108, n. 2, p. 219–232, http://dx.doi.org/10.1086/314396
Faul, H., Stern, T. W., Thomas, H. H., and Elmore, P. L. D., 1963, Ages of intrusion and metamorphism in the northern Appalachians: American Journal of Science, v. 261, p. 1–19, http://dx.doi.org/10.2475/ajs.261.1.1
Faure, G., and Mensing, T. M., 2005, Isotopes: Principles and Applications, 3rd edition: Hoboken, New Jersey, John Wiley and Sons, 897 p.
Fitzgerald, J. P., ms, 1991, Geochemistry of the Spider Lake and West Branch Penobscot volcanic suites, northern Maine: Tectonic implication from a complex petrogenesis: Boston, Massachusetts, Boston College, Master's thesis, 254 p.
Fitzgerald, J. P., and Hon, R., 1994, Mafic volcanism of the Piscataquis Volcanic Belt; B3, *in* Hanson, L., editor, Guidebook to Fieldtrips in North-Central Maine: New England Intercollegiate Geological Conference 86th Annual Meeting, September 23–25, 1994, trip B3, p. 91–122.
Fyffe, L. R., Pajari, G. E., Jr., and Cherry, M. E., 1981, The Acadian plutonic rocks of New Brunswick: Maritime Sediments and Atlantic Geology, v. 17, p. 23–36.
Fyffe, L. R., Pickerill, R. K., and Stringer, P., 1999, Stratigraphy, sedimentology and structure of the Oak Bay and Waweig formations, Mascarene Basin: implications for the paleotectonic evolution of southeastern New Brunswick: Atlantic Geology, v. 35, n. 1, p. 59–84.
Gregg, T. H., and Reusch, D. N., 2007, Geology and geochemistry of the Fish Pond Volcanics, The Forks, Maine: Geological Society of America Abstracts with Programs, v. 39, n. 1, p. 88.
Griscom, A., ms, 1976, Bedrock geology of the Harrington Lake area, Maine: Cambridge, Massachusetts, Harvard University, Ph. D. thesis, 373 p.
Hall, B. A., 1970, Stratigraphy of the southern end of the Munsungun Anticlinorium, Maine: Maine Geological Survey Bulletin B-22, 63 p., 2 pl.
Hall, B. A., Pollock, S. J., and Dolan, K. M., 1976, Lower Devonian Seboomook Formation and Matagamon Sandstone, northern Maine: A flysch basin-margin delta comples, *in* Page, L. R., editor, Contributions to the Stratigraphy of New England: Geological Society of America Memoir, v. 148, p. 57–63.
Hanson, L. S., and Bradley, D. C., 1989, Sedimentary facies and tectonic interpretation of the lower Devonian Carrabassett Formation, north-central Maine: Geological Survey of Maine Studies in Maine Geology, v. 2, p. 101–125.
Hawkins, J. W., 1994, Petrologic synthesis: Lau Basin transect (Leg 135): Proceedings of the Ocean Drilling Program, v. 135, p. 879–905, http://dx.doi.org/10.2973/odp.proc.sr.135.135.1994
Hawkins, J. W., Jr., 1995, Geology of the Lau Basin, *in* Taylor, B., editor, Backarc basins: Tectonics and magmatism: New York, Plenum Press, p. 63–138.
Hergt, J. M., and Farley, K. N., 1994, Major element, trace element, and isotope (Pb, Sr, and Nd) variations in

Site 834 basalts: Implications for the initiation of backarc opening: Proceedings of the Ocean Drilling Program, Scientific Results, v. 135, p. 471–485, http://dx.doi.org/10.2973/odp.proc.sr.135.144.1994
Hibbard, J. P., van Staal, C. R., Rankin, D. W., and Williams, H., 2006, Lithotectonic map of the Appalachian Orogen, Canada–United States of America: Geological Survey of Canada, Geological Survey of Canada "A" series map, 2 plates, scale 1:1500000
Hibbard, J. P., van Staal, C. R., and Rankin, D. W., 2010, Comparative analysis of the geological evolution of the northern and southern Appalachian orogen: Late Ordovician-Permian, *in* Tollo, R. P., Bartholomew, M. J., Hibbard, J. P., and Karabinos, P. M., editors, From Rodinia to Pangea: The Lithotectonic Record of the Appalachian Region: Geological Society of America Memoir, v. 206, p. 51–69, http://dx.doi.org/10.1130/2010.1206(03)
Holm, P. E., 1982, Non-recognition of continental tholeiites using the Ti-Y-Zr diagram: Contributions to Mineralogy and Petrology, v. 79, n. 3, p. 308–310, http://dx.doi.org/10.1007/BF00371522
Hon, R., 1980, Geology and Petrology of igneous bodies within the Katahdin pluton, *in* Roy, D. C., and Naylor, R. S. editors, A Guidebook to the Geology of Northeastern Maine and Neighboring New Brunswick: New England Intercollegiate Geological Conference Annual Meeting, p. 65–79.
Hon, R., Fitzgerald, J. P., Sargeant, S. L., Schwartz, W. D., Dostal, J., and Keppie, J. D., 1992, Silurian–early Devonian mafic volcanic rocks of the Piscataquis volcanic belt in northern Maine: Atlantic Geology, v. 28, p. 163–170.
Hubacher, F. A., and Lux, D. R., 1987, Timing of Acadian deformation in northeastern Maine: Geology, v. 15, n. 1, p. 80–83, http://dx.doi.org/10.1130/0091-7613(1987)15⟨80:TOADIN⟩2.0.CO;2
Humphreys, E., Hessler, E., Dueker, K., Farmer, G. L., Erslev, E., and Atwater, T., 2003, How Laramide-age hydration of North American lithosphere by the Farallon slab controlled subsequent activity in the western United States, *in* Klemperer, S. L., and Ernst, W. G., editors, The lithosphere of western North America and its geophysical characterization: International Geology Review, v. 45, n. 7, p. 575–595, http://dx.doi.org/10.2747/0020-6814.45.7.575
Jordan, T. E., and Allmendinger, R. W., 1986, The Sierras Pampeanas of Argentina: A modern analogue of Rocky Mountain foreland deformation: American Journal of Science, v. 286, p. 737–764, http://dx.doi.org/10.2475/ajs.286.10.737
Kay, S. M., and Abbruzzi, J. M., 1996, Magmatic evidence for Neogene lithospheric evolution of the central Andean "flat-slab" between 30°S and 32°S: Tectonophysics, v. 259, n. 1–3, p. 15–28, http://dx.doi.org/10.1016/0040-1951(96)00032-7
Kay, S. M., and Gordillo, C. E., 1994, Pocho volcanic rocks and the melting of depleted continental lithosphere above a shallowly dipping subduction zone in the central Andes: Contributions to Mineralogy and Petrology, v. 117, n. 1, p. 25–44, http://dx.doi.org/10.1007/BF00307727
Kay, S. M., Mancilla, O., and Copeland, P., 2006, Evolution of the late Miocene Chachahuén volcanic complex at 37°S over a transient shallow subduction zone under the Nequén Andes, *in* Kay, S. M., and Ramos, V. A., editors, Evolution of an Andean margin: A tectonic and magmatic view from the Andes to the Nequén Basin (35°-39°S lat.): Geological Society of America Special Paper 407, p. 215–246, http://dx.doi.org/10.1130/2006.2407(10)
Keppie, J. D., and Dostal, J., 1994, Late Silurian–Early Devonian transpressional rift origin of the Quebec Reentrant, northern Appalachians: Constraints from geochemistry of volcanic rocks: Tectonics, v. 13, n. 5, p. 1183–1189, http://dx.doi.org/10.1029/94TC01504
Kohut, E. J., and Hepburn, J. C., 2003, Movement directions and age constraints on mylonite zones near the Avalon terrane boundary NW of Boston, Massachusetts; implications for the accretion of Avalon in SE New England: Geological Society of America Abstracts with Programs, v. 35, p. 19.
Kusky, T. M., Bradley, D. C., Winsky, P., Caldwell, D. W., and Hanson, L., 1994, Paleozoic stratigraphy and tectonics, Ripogenus Gorge and nearby areas, Maine, *in* Hanson, L., editor, Guidebook to Fieldtrips in North-Central Maine: New England Intercollegiate Geological Conference 86th Annual Meeting, trip C1, p. 181–193.
Lee, C.-T. A., 2005, Trace element evidence for hydrous metasomatism at the base of the North American lithosphere and possible association with Laramide low-angle subduction: The Journal of Geology, v. 113, n. 6, p. 673–685, http://dx.doi.org/10.1086/449327
Lipman, P. W., 1992, Magmatism in the Cordilleran United States; Progress and problems, *in* Burchfiel, B. C., Lipman, P. W., and Zoback, M. L., editors, The Cordilleran Orogen: Conterminous U.S.: Geological Society of America, Decade of North American Geology, v. G-3, p. 481–514.
Marvinney, R. G., 1984, The Forks Formation of northwestern Maine: Evidence for a late Ordovician to late Silurian angular unconformity: Northeastern Geology, v. 6, p. 151–160.
McLennan, S. M., 2001, Relationships between the trace element composition of sedimentary rocks and upper continental crust: Geochemistry Geophysics Geosystems, v. 2, n. 4, paper n. 2000GC000109, 24 p., http://dx.doi.org/10.1029/2000GC000109
McMillan, N. J., and Lawton, T. F., 2006, Trigger for Laramide magmatism: normal subduction, shallow-angle subduction, or structural inheritance?: Geological Society of America Programs with Abstracts, v. 38, n. 6, p. 33.
McMillan, N. J., Lawton, T., and Cowee, C., 2003, An alternative model for Laramide magmatism in the SW US; importance of Late Jurassic continental rifting: Geological Society of America Abstracts with Programs, v. 35, p. 554.
Meschede, M., 1986, A method of discriminating between different types of mid-ocean ridge basalts and continental tholeiites with the Nb-Zr-Y diagrams: Chemical Geology, v. 56, n. 3–4, p. 207–218 http://dx.doi.org/10.1016/0009-2541(86)90004-5
Miller, D. M., Nilsen, T. H., and Bilodeau, W. L., 1992, Late Cretaceous to early Eocene geologic evolution of the U.S. Cordillera, *in* Burchfiel, B. C., Lipman, P. W., and Zoback, M. L., editors, The Cordilleran

Orogen: Conterminous U.S.: Geological Society of America, Decade of North American Geology, v. G-3, p. 205–260.
Moench, R. H., 2006, Stratigraphy of the central Maine trough from Oquossoc to Rangeley and Phillips, Maine, *in* Gibson, D., Dayl, J., and Reusch, D., editors, Guidebook for Field Trips in Western Maine: New England Intercollegiate Geological Conference, 98th Annual Meeting, p. 77–88.
Murphy, J. B., van Staal, C. R., and Keppie, J. D., 1999, Middle to late Paleozoic Acadian orogeny in northern Appalachians: A Laramide-style plume-modified orogeny?: Geology, v. 27, n. 7, p. 653–656, http://dx.doi.org/10.1130/0091-7613(1999)027⟨0653:MTLPAO⟩2.3.CO;2
Neuman, R. B., 1967, Bedrock geology of the Shin Pond and Stacyville quadrangles Penobscot County, Maine: United States Geological Survey Professional Paper 524–I, 37 p., 3 plates.
——— 1984, Geology and paleobiology of islands in the Ordovician Iapetus Ocean: Review and implications: Geological Society of America Bulletin, v. 95, p. 1188–1201, http://dx.doi.org/10.1130/0016-7606(1984)95⟨1188:GAPOII⟩2.0.CO;2
Nielsen, R. L., Landis, E. S., Ceci, V. M., and Poston, C. J., 1989, The commingling of diverse magma types in the Flagstaff Lake igneous complex, *in* Tucker, R. D., editor, Igneous and Metamorphic Geology: Augusta, Maine, Maine Geological Survey, p. 67–78.
Osberg, P. H., Hussey, A. M., III, and Boone, G. M., 1985, Bedrock Geologic Map of Maine: Augusta, Maine, Maine Geologic Survey, scale 1:500,000.
Osberg, P. H., Tull, J. F., Robinson, P., Hon, R., and Butler, J. R., 1989, The Acadian Orogen, *in* Hatcher, R. D., Thomas, W. A., and Viele, G. W., editors, The Appalachian-Ouachita Orogen in the United States: Geological Society of America, The Geology of North America, v. F-2, p. 179–232.
Pearce, J. A., 1982, Trace element characteristics of lavas from destructive plate boundaries, *in* Thorpe, R. S., editor, Andesites: New York, John Wiley and Sons, p. 525–548.
Pearce, J. A., and Cann, J. R., 1973, Tectonic setting of basic volcanic rocks determined using trace element analyses: Earth and Planetary Science Letters, v. 19, n. 2, p. 290–300, http://dx.doi.org/10.1016/0012-821X(73)90129-5
Pearce, J. A., Baker, P. E., Harvey, P. K., and Luff, I. W., 1995, Geochemical evidence for subduction fluxes, mantle melting, and fractional crystallization beneath the South Sandwich island arc: Journal of Petrology, v. 36, n. 4, p. 1073–1109, http://dx.doi.org/10.1093/petrology/36.4.1073
Pollock, S. G., 1987, The Lower Devonian slate problem of western and northern Maine revisited: Northeastern Geology, v. 9, n. 1, p. 37–50.
Pollock, S. G., Boucot, A. J., and Hall, B. A., 1988, Lower Devonian deltaic sedimentary environments and ecology: examples from the Matagamon Sandstone, northern Maine, *in* Tucker, R. D., and Marvinney, R. G., editors, Studies in Maine Geology: Structure and Stratigraphy: Maine Geological Survey, Studies in Maine Geology, v. 1, p. 81–99.
Pressley, R. A., and Brown, M., 1999, The Phillips Pluton, Maine, USA; evidence of heterogeneous crustal sources and implications for granite ascent and emplacement mechanisms in convergent orogens: Lithos, v. 46, p. 335–366, http://dx.doi.org/10.1016/S0024-4937(98)00073-5
Ramos, V. A., 2008, Field trip guide: Evolution of the Pampean flat-slab region over the shallowly subducting Nazca plate, *in* Kay, S. M., and Ramos, V. A., editors, Field trip guidebook to the backbone of the Americas in the central and southern Andes: Ridge collision, shallow subduction, and plateau uplift: Geological Society of America Field Guides 13, p. 77–116, http://dx.doi.org/10.1130/2008.0013(04)
Ramos, V. A., and Kay, S. M., 2006, Overview of the tectonic evolution of the southern Central Andes of Mendoza and Nequén (35°-39°S latitude), *in* Kay, S. M., and Ramos, V. A., editors, Evolution of an Andean margin: A tectonic and magmatic view from the Andes to the Nequén Basin (35°-39°S lat.): Geological Society of America Special Paper 407, p. 1–17, http://dx.doi.org/10.1130/2006.2407(01)
Rankin, D. W., 1968, Volcanism related to tectonism in the Piscataquis volcanic belt, an island arc of Early Devonian age in north-central Maine, *in* Zen, E.-A., White, W. S., Hadley, J. B., and Thompson, J. B., editors, Studies of Appalachian Geology: New York, Wiley Interscience, p. 355–369.
——— 1994, Early Devonian explosive silicic volcanism and associated early and middle Devonian clastic sedimentation that brackets the Acadian Orogeny, Traveler Mountain area, Maine, *in* Hanson, L., editor, Guidebook to Fieldtrips in North-Central Maine: New England Intercollegiate Geological Conference 86th Annual Meeting, p. 135–157.
Rankin, D. W., and Hon, R., 1987, Traveler Rhyolite and overlying Trout Valley Formation and Katahdin pluton; a record of basin sedimentation and Acadian Magmatism, north-central Maine, *in* Roy, D. C., editor, Geological Society of America Centennial Field Guide—Northeastern Section: Geological Society of America, v. 5, p. 293–301.
Rankin, D. W., and Tucker, R. D., 1995. U-Pb age of the Katahdin-Traveler igneous suite, Maine, local age of the Acadian Orogeny, and thickness of the Taconian crust: Geological Society of America Abstracts with Programs, v. 27, p. A-224.
Reusch, D. N., and van Staal, C. R., 2011, The Dog Bay–Liberty Line and its signficance for Silurian tectonics of the northern Appalachian orogen: Canadian Journal of Earth Sciences.
Robinson, P., 1993, Acadian magmatism and metamorphism in New England: a product of mantle-lithosphere delamination in front of an east-dipping subduction zone?: Geological Society of America Abstracts with Programs, v. 25, n. 6, p. A–179.
Robinson, P., Tucker, R. D., Bradley, D., Berry, H. N., IV, and Osberg, P. H., 1998, Paleozoic orogens in New England, USA: GFF, v. 120, p. 119–148.
Rollinson, H., 1993, Using geochemical data: evaluation, presentation, interpretation: Essex, Prentice Hall, 352 p.
Samson, S. D., Hibbard, J. P., and Wortman, G. L., 1995, Nd isotopic evidence for juvenile crust in the Carolina terrane, southern Appalachians: Contributions to Mineralogy and Petrology, v. 121, n. 2, p. 171–184, http://dx.doi.org/10.1007/s004100050097

Samson, S. D., Barr, S. M., and White, C. E., 2000, Nd isotopic characteristics of terranes within the Avalon Zone, southern New Brunswick: Canadian Journal of Earth Sciences, v. 37, n. 7, p. 1039–1052, http://dx.doi.org/10.1139/e00-015

Saunders, A. D., and Tarney, J., 1984, Geochemical characteristics of basaltic volcanism within back-arc basins, *in* Kokelaar, B. P., and Howells, M. F., editors, Marginal basin geology: volcanic and associated sedimentary and tectonic processes in modern and ancient marginal basins: Geological Society, London, Special Publications, v. 16, p. 59–76, http://dx.doi.org/10.1144/GSL.SP.1984.016.01.05

Saunders, A. D., Norry, M. J., and Tarney, J., 1988, Origin of MORB and chemically-depleted mantle reservoirs; trace element constraints, *in* Menzies, M. A., and Cox, K. G., editors, Oceanic and continental lithosphere: Similarities and differences: Journal of Petrology Special Volume 1988, p. 415–445, http://dx.doi.org/10.1093/petrology/Special_Volume.1.415

Schoonmaker, A., and Kidd, W. S. F., 2006, Evidence for a ridge subduction event in the Ordovician rocks of north-central Maine: Geological Society of America Bulletin, v. 118, n. 7–8, p. 897–912, http://dx.doi.org/10.1130/B25867.1

Schoonmaker, A., Kidd, W. S. F., and Bradley, D. C., 2005, Foreland-forearc collisional granitoid and mafic magmatism caused by lower-plate lithospheric slab breakoff: The Acadian of Maine, and other orogens: Geology, v. 33, n. 12, p. 961–964, http://dx.doi.org/10.1130/G21832.1

Shervais, J. W., 1982, Ti-V plots and the petrogenesis of modern and ophiolitic lavas: Earth and Planetary Science Letters, v. 59, n. 1, p. 101–118, http://dx.doi.org/10.1016/0012-821X(82)90120-0

Simmons, R. H., 1987, Bedrock geology of portions of the North East Carry and Moosehead Lake quadrangles, Maine: Maine Geological Survey Open File Report n. 87–22, 17 p., 1 map.

Sun, S.-s. and Mcdonough, W. F., 1989, Chemical and isotopic systematics of oceanic basalts: implications for mantle composition and processes, *in* Saunders, A. D., and Norry, M. J., editors, Magmatism in the Ocean Basins: Geological Society, London, Special Publications, v. 42, p. 313–345, http://dx.doi.org/10.1144/GSL.SP.1989.042.01.19

Thompson, J. F. H., 1984, Acadian synorogenic mafic intrusions in the Maine Appalachians: American Journal of Science, v. 284, p. 462–483, http://dx.doi.org/10.2475/ajs.284.4-5.462

Tucker, R. D., Osberg, P. H., and Berry, H. N., IV, 2001, The geology of a part of Acadia and the nature of the Acadian Orogeny across central and eastern Maine: American Journal of Science, v. 301, p. 205–260, http://dx.doi.org/10.2475/ajs.301.3.205

van der Velden, A. J., van Staal, C. R., and Cook, F. A., 2004, Crustal structure, fossil subduction and the tectonic evolution of the Newfoundland Appalachians: Evidence from a reprocessed seismic reflection survey: Geological Society of America Bulletin, v. 116, n. 11–12, p. 1485–1498, http://dx.doi.org/10.1130/B25518.1

van Staal, C. R., 2007, Pre-Carboniferous tectonic evolution and metallogeny of the Canadian Appalachians, *in* Goodfellow, W. D., editor, Mineral Deposits of Canada: A Synthesis of Major Deposit-types, District Metallogeny, the Evolution of Geological Provinces, and Exploration Methods: Geological Association of Canada, Mineral Deposits Division, Special Publications, v. 5, p. 793–818.

van Staal, C. R., and de Roo., J. A., 1995, Mid-Paleozoic tectonic evolution of the Appalachian Central Mobile Belt in northern New Brunswick, Canada: collision, extensional collapse, and dextral transpression, *in* Hibbard, J. P., van Staal, C. R., and Cawood, P. A., editors, Current Perspectives in the Appalachian-Caledonian Orogen: Geological Association of Canada Special Paper, v. 41, p. 367–389.

van Staal, C. R., Whalen, J. B., Valverde-Vaquero, P., Zagorevski, A., and Rogers, N., 2009, Pre-Carboniferous, episodic accretion-related, orogenesis along the Laurentian margin of the northern Appalachians, *in* Murphy, J. B., Keppie, J. D., and Hynes, A. J., editors. Ancient orogens and modern analogues: Geological Society, London, Special Publications, v. 327, p. 271–316, http://dx.doi.org/10.1144/SP327.13

Waldron, J. W. F., Murphy, J. B., Melchin, M. J., and Davis, G., 1996, Silurian tectonics of western Avalonia; strain-corrected subsidence history of the Arisaig Group, Nova Scotia: The Journal of Geology, v. 104, n. 6, p. 677–694, http://dx.doi.org/10.1086/629862

Weaver, S. D., Saunders, A. D., Pankhurst, R. J., and Tarney, J., 1979, A geochemical study of magmatism associated with the initial stages of back-arc spreading; the Quaternary volcanics of Bransfield Strait, from South Shetland Islands: Contributions to Mineralogy and Petrology, v. 68, n. 2, p. 151–169, http://dx.doi.org/10.1007/BF00371897

Wells, M. L., and Hoisch, T. D., 2008, The role of mantle delamination in widespread Late Cretaceous extension and magmatism in the Cordilleran orogen, western United States: Geological Society of America Bulletin, v. 120, n. 5–6, p. 515–530, http://dx.doi.org/10.1130/B26006.1

West, D. P., Jr., Tomascak, P. B., Coish, R. A., Yates, M. G., and Reilly, M. J., 2007, Petrogenesis of the ultrapotassic Lincoln Syenite, Maine: Late Silurian–Early Devonian melting of a source region modified by subduction driven metasomatism: American Journal of Science, v. 307, p. 265–310, http://dx.doi.org/10.2475/01.2007.08

Whalen, J. B., McNicoll, V. J., van Staal, C. R., Lissenberg, C. J., Longstaffe, F. J., and Jenner, G. A., and van Breeman, O., 2006, Spatial, temporal and geochemical characteristics of Silurian collision-zone magmatism, Newfoundland Appalachians; an example of a rapidly evolving magmatic system related to slab break-off: Lithos, v. 89, n. 3–4, p. 377–404, http://dx.doi.org/10.1016/j.lithos.2005.12.011

White, C. E., Barr, S. M., Reynolds, P. H., Grace, E., and McMullin, D. W. A., 2006, The Pocologan metamorphic suite: high-pressure metamorphism in a Silurian fore-arc complex, Kingston Terrane, southern New Brunswick: The Canadian Mineralogist, v. 44, n. 4, p. 905–927, http://dx.doi.org/10.2113/gscanmin.44.4.905

Winchester, J. A., and Floyd, P. A., 1977, Geochemical discrimination of different magma series and their differentiation products using immobile elements: Chemical Geology, v. 20, p. 325–343, http://dx.doi.org/10.1016/0009-2541(77)90057-2

Winchester, J. A., and van Staal, C. R., 1994, The chemistry and tectonic setting of Ordovician volcanic rocks in northern Maine and their relationship to contemporary volcanic rocks in northern New Brunswick: American Journal of Science, v. 294, p. 641–662, http://dx.doi.org/10.2475/ajs.294.5.641
Wintsch, R., Aleinikoff, J., Dorais, M., Walsh. G., and Kunk, M., 2008, The case for crustal wedging in the assembly of the southern New England Appalachians: International Geological Congress, Abstracts, v. 33, Abstract 1337985.
Wood, D. A., 1980, The application of a Th-Hf-Ta diagram to problems of tectomagmatic classification and to establishing the nature of crustal contamination of basaltic lavas of the British Tertiary Volcanic Province: Earth and Planetary Science Letters, v. 50, n. 1, p. 11–30, http://dx.doi.org/10.1016/0012-821X(80)90116-8
Wood, D. A., Joron, J.-L., and Treuil, M., 1979, A reappraisal of the use of trace elements to classify and discriminate between magma series erupted in different tectonic settings: Earth and Planetary Science Letters, v. 45, n. 2, p. 326–336, http://dx.doi.org/10.1016/0012-821X(79)90133-X
Yuan, C., Min, S., Wilde, S., Xiao, W., Xu, Y., Long, X., and Zhao, G., 2010, Post-collisional plutons in the Balikun area, East Chinese Tianshan: Evolving magmatism in response to extension and slab break-off: Lithos, v. 119, p. 269–288, http://dx.doi.org/10.1016/j.lithos.2010.07.004